FACULDADE DE ENGENHARIA DA UNIVERSIDADE DO PORTO

TexSense: Sistema de monitorização Wearable para vestuário de desporto

Ana Rita Gouveia

Integrated Master in Bioengineering

Supervisor: Miguel Velhote Correia, PhD

October 22, 2019

TexSense: Sistema de monitorização Wearable para vestuário de desporto

Ana Rita Gouveia

Integrated Master in Bioengineering

October 22, 2019

Resumo

O processo de conceção e o desenvolvimento de roupa de desporto é um processo altamente complexo que envolve um elevado gasto de recursos, que vão desde matérias-primas e gastos com a maquinaria à mão-de-obra. Para além disso, é necessário criar vários protótipos intermédios até obter um protótipo que vá de encontro às necessidades do atleta. Como se não bastasse, não existe uma medida objetiva para a avaliação de cada protótipo, o que pode levar a erros na avaliação dos mesmos.

Deste modo, o objetivo deste projeto inovador é criar uma ferramenta, constituída por um fato vestível e uma aplicação móvel, que permita a digitalização e desmaterialização de protótipos. Consequentemente, esta dissertação teve como objetivo o desenvolvimento de um sensor de extensão que será integrado no fato vestível.

Diferentes têxteis/materiais, disponibilizados pelo CITEVE, foram testados e uma solução baseada em pasta de carbono condutiva mostrou ser a melhor opção. A solução encontrada tem alta linearidade, relativamente alta sensibilidade, baixa histerese e tempo de resposta. Para além destas excelentes características, como a pasta condutora de carbono é imprimida no têxtil, o movimento do atleta não é comprometido. Desenharam-se e testaram-se dois circuitos eletrónicos com a função de comunicar com o módulo central. Por fim, desenvolveu-se uma aplicação web capaz de comunicar com o sensor de extensão, uma vez que, em certas aplicações, pode ser vantajoso usar, individualmente, o sensor de extensão. Esta aplicação é facilmente escalável e algumas funcionalidades podem ser adicionadas, de acordo com a aplicação do sensor.

Palavras-chave: *Sensores de extensão flexíveis, sensores resistivos, dispositivos vestiveis, pasta condutora de carbono*

Abstract

The design and development of sportswear is a highly complex process that consumes a lot of resources, ranging from raw materials and machinery to human resources. Besides this, several intermediate prototypes need to develop until it meets the athlete's needs. As if that were not enough, there is not an objective measure for prototype evaluation, which could result in evaluation errors.

Therefore, this innovative project aims to create a tool that consists of a wearable device and a mobile application to allow a prototype digitalization and dematerialization. Consequently, the goal of this dissertation was to develop a stretchable strain sensor to be integrated into this wearable monitoring system.

Several textiles/materials provided by CITEVE were tested and a solution based on a carbon conductive paste was considered the best option. This new solution found presents high linearity, relatively high sensitivity, low hysteresis and response time. Besides these excellent characteristics, the conductive paste is printed on the textile, therefore, it does not compromise the athletes' movements. Also, two circuits were designed and tested to communicate with the core module. Besides the above, it was decided to develop a prototype of a web application capable of communicating with the built sensor since in some applications it may be worthwhile to use the strain sensor individually. This web app can be easily scalable and some features easily added according to the strain sensor application.

Keywords: *Stretchable strain sensor, resistive sensors, wearable devices, carbon conductive paste*

Agradecimentos

Não podia começar sem agradecer às pessoas que mais contribuíram para esta dissertação: ao meu orientador, Prof. Miguel Velhote Correia, pelo acompanhamento e paciência, e ao Waldri, que apesar de não ter qualquer obrigação, sempre se disponibilizou para me ajudar.

Em seguida, aos meus pais, que para além de serem duas das pessoas mais importantes da minha vida são também os responsáveis por estar prestes a concluir mais um capítulo. Obrigada por todo o apoio e todos os esforços que fizeram para eu poder estar aqui hoje. Não podia deixar de agradecer também à minha irmã, que apesar de insuportável às vezes, foi também o meu maior pilar ao longo de todos estes anos.

Gostava também de agradecer às duas pessoas mais importantes que conheci na FEUP: Bruno e Nina. Obrigada por todos os planos, gargalhadas, conversas e por nunca me deixarem de apoiar, mesmo quando desabafava 10000 vezes e o assunto era sempre o mesmo.

Ao Paulo e à Marina, dois anjos super altruístas caídos do céu que escrevem sebentas, o maior obrigado do mundo: também pelas sebentas, mas principalmente por toda a amizade e por serem as excelentes pessoas que são.

Por tornarem as minhas quartas (e os outros dias da semana) menos vulgares, um agradecimento especial ao grupo das quartas-feiras (ao Bruno -outra vez-, à minha Rafinha, ao Dudu, à Joana (Ju), à Api e à Varejão).

Um agradecimento à Joana (JAD) por se ter tornado tão importante nos últimos três anos e à Maggie por todas as conversas sobre "tragédias" do passado e por me ter proporcionado dos melhores momentos na faculdade – o dilúvio sobre 4 rodas.

Não menos importantes, os meus amigos de Lamego, principalmente a Juju, Lili e Teté que agora não vejo com a frequência que desejava.

Ah, e já me esquecia, ao meu namorado (eu sei que isto não fica bem aqui, mas apostas são apostas!).

Ana Rita Gouveia

"Fall in love with becoming the best version of yourself but with patience, with compassion and respect to your own journey"

s.mcnutt

Contents

List of Figures

List of Tables

Abbreviations

CNT	Carbon Nanotube
CCP	Carbon Conductive Paste
ECG	Electrocardiography
EEG	Electroencephalography
GF	Gauge Factor
GPS	Global Positioning System
ICPs	Inherently Conductive Polymers
I^2C	Inter-Integrated Circuit
LED	Light Emitting Diode
SCL	Serial Clock
SDA	Serial Data
UI	User Interface
UP180+b	U-shaped P180+b
W1	Wire (1st configuration)
W2	Wire (2nd configuration)
VJ	Vital Jacket

Chapter 1

Introduction

1.1 Context and Motivation

The design and development of sportswear is a very complex process that involves continuous efforts at prototype improvement until it meets the athlete's needs. [26]

This process begins with athlete's clothing measurements. This is followed by meetings with the athlete to identify his needs, choosing the appropriate materials, developing the 2D clothing patterns, preparing the raw materials to be used, cutting and sewing garments using textile company's technologies.

Once the prototype is ready, a test is performed in a real world environment. In this test, measurements are taken and inquiries are made to the athlete in order to validate the prototype's performance and optimize its shape and fitting by identifying the necessary improvements and the reengineering to be made in a new prototype.

Besides that there is another problem: there is no reliable and objective measure of athlete's needs, resulting in a loss of information. For example, the degree of compression of garments and their ability to release heat are very important factors to be considered. However, the textile company does not own a technology capable of objectively evaluating these parameters. This makes all the responsibility lies with the athlete's opinion that could not always be the most assertive and can have a negative impact on the evaluation of the prototype. As a result, in most cases, it is required an almost total redesign of prototype and several prototypes to obtain a final product.

This implies both an over-exploitation and an inefficient use of resources. Therefore, a tool capable of reducing the waste of textile companies resources would be worthwhile.

1.2 Problem Definition and Objectives

As a way to reduce resource waste in sportswear development, it is intended to create a innovative tool for prototype digitalization and dematerialization through wearable technology.

Wearables, specially smart garments, can monitor users during their tasks without compromising their comfort, which makes wearable technology a very useful tool for sports monitoring [1].

Therefore, the main objective of the project TexBoost-PPS1 Digitalization and Desmaterialization is to create a tool capable of generating objective and reliable information for the development and validation of cyclists' equipment that does not require the production of several prototypes saving time and money. This tool will be developed by FEUP, INESC TEC, CITEVE, FADEUP, LABIOMEP, P&R Têxteis, LMA and PLUX and it consists of a smart garment and a mobile application.

The smart garment will require technology that includes motion capture and biomechanic sensors to get information related to athlete's body movements. However, this dissertation focuses on the development of the strain sensors since the other sensors of the wearable system are being developed by PLUX. Strain sensors will be needed to monitor body sites capable of withstanding large strains.

The information collected by the smart garment will be sent to the mobile app and it will be converted into objective data needed for final product development.

1.3 Dissertation Structure

Besides this Introduction, this dissertation presents seven more chapters.

Chapter 2 focuses on wearable technology: the topics approached are smart garments and smart textiles, their evolution, classification, materials and fibers, components and fields of application. Besides this, some examples of commercially available solutions are present. The trends of the wearable market, in which the smart garments market is included, is also a topic covered in this chapter.

In Chapter 3, strain sensors for textile integration are the main topic. It starts by explaining their operating principle, followed by the principal measures for performance evaluation, some prototypes, commercially available solutions and applications.

Chapter 4 reports all the stages necessary for the strain sensor textile selection (test, data preprocessing, analysis of the results).

Chapter 5 discusses the design of the sensor electronic circuit capable of communicating with the core module.

Chapter 6 shows a prototype of a web application capable of receiving the sensor data and save it for multiple measurements in a proper and organised manner.

Finally, Chapter 7 presents all the conclusions obtained during this work and some suggestions for future work.

Chapter 2

Wearable Devices

A wearable device is an electronic device closely attached to the user's body, worn under, with or on top of clothing that can acquire, store and process data. Two types of wearable devices can be distinguished: wearable gadgets and smart garments [1].

Wearable gadgets are computing devices such as fitness bracelets or eyewear computers that are strapped to certain parts of the body. Therefore, wearable gadgets need to be attached, removed and the user can forget or choose not to use them. The device is always seen as an extension to the user.

In contrast to wearable gadgets, smart garments also known as e-garments are clothes built using smart textiles with electronics embedded allowing the incorporation of technology in everyday clothes. As can be seen in Fig.2.1, e-garments are the result of the fusion of wearable technology and functional textiles.

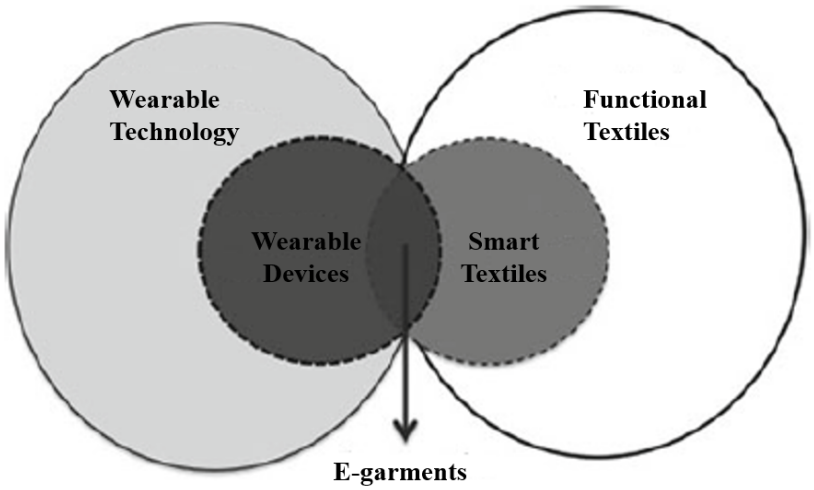

Figure 2.1: E-garments as a combination of wearable technology and functional textiles [1].

2.1 Smart textiles and smart garments

Smart textiles are fabrics that can sense stimulus and external conditions, respond and even adapt themselves to the stimulus and conditions. These stimuli can cover several types: mechanical, thermal, electrical, magnetic, optical, etc [27]. Smart textiles can provide information about users and their everyday lives playing an important role in non-invasive and continuous monitoring. For this reason, they present a big challenge in various fields of application such as sports, automotive, health, medical, military, aerospace, etc.

2.1.1 Evolution of Smart Textiles and Smart Garments

The main materials needed for the development of e-textiles, threads, and fabric with conductive abilities have been available for more than 1000 years [28].

For centuries, artisans have been making textiles using fine metal foils like gold and silver wrapped around fabrics threats. As an example, many of Queen Elizabeth I's gowns, which date back to the 16th century, had gold-wrapped threads embroidered.

In the late 19th century, designers and engineers began working together and developing clothing and jewelry combined with electricity such as enlightened and motorized necklaces, hats, and costumes. A good example of this is the young women adorned in light-studded evening gowns from Electric Girl Lighting Company hired to provide cocktail party entertainment in the late 1800s.

In 1968, an innovative exhibition called "Body Covering" [2] focused on the link between technology and apparel were organized by the Museum of Contemporary Craft, located in New York. In this exhibition, astronauts' space suits along clothing capable of inflating and deflating, heating, cooling and lighting up itself were exposed (see Fig. 2.2 for some examples of these garments).

(a) (b) (c)

Figure 2.2: Some garments of "Body Covering" exhibition. (a) Block II Apollo pressure suit (left). New Apollo pressure suit, covered with a layer of Beta fabric (non-flammable fiberglass cloth) (right); (b) Cooling suit, lined with a network of flexible vinyl tubing to circulate water as a heat transfer fluid; (c) Electrically heated garment. Adapted from [2].

Fig. 2.3 shows some garments (electroluminescent dress and jacket and a belt that could sound alarm sirens) made by Diana Drew, one of the designers of the collection presented in this exhibition.

(a) (b) (c)

Figure 2.3: Some clothing garments of Diana Dew's collection. (a) "Movie Dress", leather with illuminated photographs, operated by self-contained power-pack; (b) "Motorcycle jacket", leather with silk lining electroluminescent and incandescents lights operated by self-contained power-pack; (c) Belt with mounted speaker for alarm and communication. Adapted from [2].

In 1985, Harry Wainwright realized he could add animation to apparel. Thus, he created the first fully animated sweatshirt with optic fiber, light emitting diodes (LEDs) and a microprocessor. The microprocessor could control single frames of the animation and, therefore, create full-color cartoon animations. In order to be able to manufacture plastic optical fibers (POF) embedded fabrics for mass smart markets, in a partnership with Herbert Selbach – german designer- he created the world's first computer numeric control (CNC) machine, in 1997. The CNC machine started producing animated coats for Disney Parks, in 1998 [29].

In the middle of the years 1990, a team of Massachusetts Institute of Technology (MIT) researchers led by Steve Mann, Thad Starner, and Sandy Pentland started developing what they called wearable computers. Another MIT group was responsible for exploring a better integration of these devices into clothing and soft substrates.

In 1999, it was created the sensor jacket- one of the first textile-based wearable computers. It consists of a smart garment that measures upper body posture with a knitted stretch sensor put over the joints [30]. Since then sensors have been the subject of several publications:

- A yarn sensor nearly free of hysteresis was analyzed for measure elongation of body parts [31];
- Different conductive textiles and their performance for measuring joint angles were evaluated [32];
- A textile strain was used to measure the flexing angle and showed that there is a linearity between its resistance and the flexing angle [33], etc;

In 2005, Wainwright and David Bychkov create the first electrocardiography (ECG) Bio-Physical display jacket with LED/Optic display and galvanic skin response sensors in a watch connected with the denim smart jacket via Bluetooth. A year later, Wainwright unveiled additional smart fabric technologies at The Smart Fabric Conference in Washington, DC. One of the most interesting technologies shown was an infrared digital display embedded in the fabric for identification of friend or foe [29].

Many research projects started to focuses on the physiological status of the wearer:

- A smart garment that could be used as wearable healthcare system was presented [34];
- In the multinational European MyHeart project it was developed underwear to be used for cardiovascular diseases that measure ECG, respiration and several other measurements [35];
- A system for cardiorespiratory measurement condition during sleep was presented [36];
- An ECG shirt was developed and several types of integration were compared [32];
- A belt-worn sensor to measure respiratory cycle and respiration rate (RR)- wave interval using conductive fabric was designed, etc.

2.1.2 Classification of smart textiles

Depending on the way they take action in the presence of a stimulus, smart textiles can be divided into three categories: passive smart, active smart and intelligent textiles. According to their category, three different components may be presented: sensors, actuators, and controlling units [7].

Passive smart textiles are materials that can only detect stimulus or changes in the environment. Therefore, sensors are essential in passive smart materials.

Active smart textiles are materials that cannot only sense stimulus but also respond to them. In order to do that, they need a sensor that detects a stimulus, an actuator that responds directly to the detected signal or indirectly from a central control unit.

Intelligent materials also known as very smart materials are materials that are able to sense, react and even to adapt themselves. These materials, besides sensors, actuators and controlling units, require another unit responsible for cognition, reasoning and activating capacities.

Aside from this division, there is another made in [37] based on the degree of use of textiles as electronic components. According to this division, there are also three categories of smart textiles.

In the first category, smart textiles are used to integrate off-the-shelf electronic components. The cables that connect sensors, actuators or processing boards are replaced for conductive yarns and fibers.

In the second category, electronics start being replaced by textiles. Textiles can work as sensors or actuators. Thus, there are only some parts that are composed of traditional electronics.

The third category consists of textiles that do not include electronics, so logic boards, transistors, and other electronic components are made out of textiles.

2.1.3 Materials and fibers in smart textiles

Sensors or connection substrates have been developed using metal fibers, conductive inks, inherently conductive polymers, electrically conductive textiles, optical fibers, coatings with nanoparticles, shape memory, chromic and phase change materials [28]. Each material will be briefly discussed in the next sections.

2.1.3.1 Metal fibers

Metal threads are made of thin metal fibers produced by the bundle-drawing process or shaving process in which the edge of the thin metal sheeting is shaved. The threads and yarns are knitted or woven into the fabric and they are used to interconnects components. Besides that, some ECG signals are obtained by electrodes made of these metal fibers.

2.1.3.2 Conductive inks

Conductive inks can be used to create a layout that adds conductivity to some areas of the garment. Carbon, copper, silver, and gold are some of the materials that can be mixed with regular printing inks to turn them conductive.

2.1.3.3 Inherently conductive polymers (ICPs)

ICPs have sensing and actuating properties. The most suitable is Polypyrrole that has a high mechanical strength, high elasticity, and stability when it is in contact with air. Although these materials present several advantages such as the retention of the natural structure of the material, they have disadvantages regarding the resistance variation over time and high response time.

2.1.3.4 Electrically conductive textiles

For years electrically conductive textiles have been used to control electromagnetic interference shielding. These materials provide good electrical conductivity and they can be used in smart textiles as electrodes or interconnects between components.

2.1.3.5 Optical Fibers

Optical fibers are easily integrated into textiles and they are a good option since they do not generate heat and are not sensitive to electromagnetic radiation. They play several roles in smart garments, from the transmission of the data signal to the detection of deformations in fabrics. Luminex® fabric is commercially available textile with woven optical fibers that have the ability to emit light.

2.1.3.6 Coating with nano-particles

Coating fabric with nanoparticles can improve textile performance and functionality. Coating with nano-particles enhance some characteristics of the textiles such as water-repellence, UV protection without change some beneficial properties like self-cleaning and tactile properties.

2.1.3.7 Shape memory materials

A shape memory alloys have different properties below and above the temperature of activation and they are used to increase the protection against heat sources. The same effect occurs with shape memory polymers but they present an advantage: as polymers, they tend to be more compatible with textiles than alloys.

2.1.3.8 Chromic materials

Chromic materials can change their colors in the presence of a certain stimulus. Depending on the stimuli type, they have different categories:

- Photo chromic: light is the external stimulus;
- Thermo chromic: heat is the external stimulus;
- Electro chromic: electricity is the external stimulus;
- Piezoro chromic: pressure is the external stimulus;
- Solvate chromic: liquid or gas is the external stimulus;

They are usually used in fashion to create color-changing designs.

2.1.3.9 Phase change materials

Phase change materials are highly used nowadays in several fields of textile applications: anti-ballistic vest, automotive, medical, etc. The quality that makes the application of phase change materials in smart textiles interesting is their ability to store heat and release it whenever necessary. Therefore, it is possible to produce protecting garments to be used in all kind of weathers.

2.1.4 Components of Smart Garments

Sensing, actuation, control, communications, and power subsystems are the most common in smart garments [3]. Fig.2.4 shows the basic structure of a smart garment system.

These subsystems communicate via wireless or by using conductive fabrics. Anyway, it is crucial to have in mind that this interconnection is essential to the wearability, reliability, washability, and miniaturization of a smart textile.

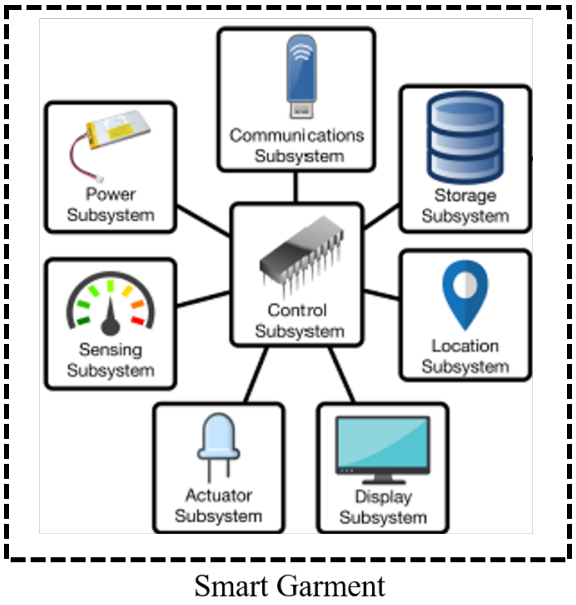

Figure 2.4: Basic structure of an internet of things (IoT) smart garment system [3].

2.1.4.1 Sensing subsystems

Sensing subsystem can be made by several types of sensors capable of sensing different stimuli or phenomena from its surroundings. According to what sensors monitor, they have different categories. The most common are:

- Vital signs sensors: these type of sensors are used to monitor heart rate, respiration rate, blood pressure, pulse oxygenation, glucose levels, and obtain some biometrics such as ECG and electroencephalography (EEG).
- Motion, gesture, and position: the most adopted sensors for these functions are accelerometers and gyroscopes. Barometers can be used in few applications to get user's altitude. Other motion sensors, although less used, are tilt-switches, vibration sensors or body pedometers.
- Location: Positioning outdoors is easily through GPS. It allows identifying the user's position by using the distance from at least three satellites in an accurate and low resourcing way. However, this technology is not a feasible solution for indoor positioning that demands other location techniques such as received signal strength indicator (RSSI) combined with the direction of arrival (DoA). [38]
- Body temperature: To measure body temperature, thermistors or resistance temperature detectors (RTDs) are used.
- Interaction: Mechanical and tactile switches sensors are capable of sensing touch. Besides this, there are also capacitive or resistive touchscreens, textile switches, etc.

2.1.4.2 Actuation subsystems

Actuators permit smart garments to react to stimuli. The most used actuators in smart garments are:

- Visual indicators: They emit light and visual information by LEDs, optical fiber, liquid-crystal display (LCDs) or electronic-inks display.
- Sound: These actuators emit sound and voice through loudspeakers, buzzers, earphones, etc.
- Movement and vibration: they are capable of transform electricity into movement. An example of this type of actuators is electric and vibration motors.
- Cooling and heating: Resistive heaters are able to function as heaters and thermoelectric materials as coolers.

2.1.4.3 Control subsystems

The control subsystem can be developed using different types of electronic devices. For example, we have central processing units (CPUs), microcontrollers, field-programmable gate arrays (FPGAs) and Systems-on-a-Chip (SoCs). Their advantages and disadvantages can be found on table 2.1.

2.1.4.4 Communications subsystems

This subsystem has two main tasks: data exchanges between a communications gateway and the smart garment and user's identification.

For short distances, radio-frequency identification (RFID) technology [39] can be used to provide the user's identifier. Through radio transponders also known as tags, a unique identifier and, perhaps, some information is emitted. Then, it is necessary to use an RFID reader. This technology is advantageous because the tag and the reader do not need to be in the line-of-sight and, for some short distances, tags do not require batteries. Near Field Communication (NFC) [40] - widely used in Android's phones [41]- can also be used for short distances and it provides better results than RFID technology.

Since most of the smart garments need to be capable of communication with smartphones, 3G/4G, Wi-Fi and Bluetooth are used. Bluetooth low energy (BLE) is a new low energy version of Bluetooth and it can be used instead Bluetooth to enable communication with lower power consumption. Similarly, HaLowIEEE 802.11ah is a Wi-Fi technology with long range and low power.

Table 2.2 shows the frequency band, maximum range, data rate and power features of some of the most used wireless technologies.

Table 2.1: Types of controllers, a brief description and their advantages and disadvantages. Adapted from [3, 20, 21, 22].

Type of Controller	Brief Description	Advantages	Disadvantages
CPU	A component capable of calculating and realizing tasks determined by the user. It is the main component of the computer hardware.	- High computational power.	- Consume too much energy.
Microcontroller	Small computer combined in a single integrated circuit.	- Consume less energy; - Capable of being easily reprogrammed; - Processing power is enough to execute the tasks.	- It imposes limitations on the size of data; - It may over-heat.
FPGA	A semicustom integrated circuit that can be field-programmed.	- Good performance; - Capable of being easily reprogrammed with a different design according to the application	- Design development may not be straightforward; - Consume too much energy
ASIC	Integrated circuit design for a particular purpose.	- Designed according to their application; - Perform specific tasks faster and minimized power consumption because they are optimized for given tasks	- Costly, so it is only worthwhile when a high number of devices will be developed.
SoC	An integrated circuit that combines every part of a computer into a chip	- Space-saving makes it great for integration; - High manufacturing costs; - More power efficient than systems with separated components;	- High manufacturing costs

Table 2.2: Some of the most used wireless technologies for communication, a brief description, their frequency band, maximum range, data rate and power/main features. Adapted from [3, 23, 24, 25].

Technology	Brief Description	Frequency Band	Maximum Range	Data Rate	Power/Main Features
UHF RFID	Ultra-high frequency RFID	30 MHz–3GHz	tens of meters	<640 kbit/s	Non-line-of-sight, durability, low cost
NFC	Near-field communication protocols to allow communication between two devices	13.56MHz	<20 cm	424 kbit/s	Low cost, no power
3G	Third generation technology of wireless mobile telecommunications	1920–1975 MHz	Up to 100km	384 kbits/s - 10 Mbit/s	Affordable, long distance
4G	Fourth generation technology of wireless mobile telecommunications	2500–2690 MHz	Up to 100km	3- 100 Mbit/s	Affordable, long distance
Wi-Fi HaLow/IEEE 802.11ah	Low power, long range Wi-Fi	868–915MHz	<1 km	100 Kbit/s per channel	Low power
Bluetooth 5 Low Energy (BLE)	Bluetooth's latest low energy version	2.4GHz	<400m	1360 kbit/s	Low power and rechargeable
LoRa	Long range wireless data communication technology	2.4 GHz	kilometers	0.25–50 kbit/s	Long battery life and range
UWB/IEEE 802.15.3a	Ultra wideband technology	3.1 to 10.6 GHz	<10 m	>110 Mbit/s	Low power, rechargeable (hours to days)
ZigBee	short-range wireless networking standard	868–915 MHz, 2.4 GHz	<100 m	20–250 kbit/s	Very low power (batteries last months to years), up to 65,536 nodes

2.1.4.5 Power subsystems

Depending on the power devices consume, they can be classified as low-end, mid-range and high-end devices.

Low-end devices are devices with low energy consumption and can last for long periods without being recharged (e.g., pacemakers or analog watches).

Mid-range devices consume an average of 500mW and can last almost a day without being recharged (e.g., portable radio).

High-end devices use up to 50 Watts (e.g., smartphones and laptops).

According to their category, they need different types of battery. Low-end devices use button-type batteries; medium range devices use bulkier batteries such as AA or AAA that are less appropriated to be used in garments, and high- end devices usually use Li-ion batteries which are heavy and increase the garment's weight [3].

Regarding the power consumption in smart garments topic, many attempts to increase the flexibility and lightning of batteries have been made. Besides this, it were created full cells through printing-based methods [42].

Energy harvesting solutions have also been a subject of studies such as harvesting energy through the human body's motion [43] and heat [44] or renewable resources like the sun or wind [45].

Concerning the recharge method, recharge can be done by waterproof universal serial bus (USB) connections and direct current (DC)-power jacks and even through wireless recharging batteries [46].

2.1.5 Fields of Application

Smart garments have several fields of application. Healthcare, sports, security, military, fashion articles are some examples that will be discussed in more detail in this section.

2.1.5.1 Heathcare

The development of smart garments that allows continuous monitoring play an important role in healthcare, more precisely, in telemedicine. The monitoring of bio-signals has been very active in healthcare. As bio-signals are dynamic, continuous monitoring provides better insight into patient health. This is essential to overcome the problem of infrequent clinical visits where the physician only has access to a brief window of the patient's health condition [28].

Heart rate monitoring can be used to infer about cardiovascular diseases.

Blood pressure monitoring can be used to detect abnormal risings on the pressure that could result in strokes and another organ damage [7].

Other biometrics such as ECG, EMG, EEG, physical stress levels, breathing patterns are usually monitored [3].

Smart garments are also used to detect movement patterns. Since motor functions are affected by some neurological disorders, analyzing the patient's movement patterns have great value not only in the routine clinical care but also in trials for new therapies.

The control of body posture is another functionality of smart garments and have a significant interest in rehabilitation and sports medicine.

2.1.5.2 Sports

In sports, smart garments are used in sportswear to evaluate athletes' condition and performance. Some of their functionalities are monitoring heart, body temperature, elongation; stimulates muscles; record their performance parameters and protect them against injuries.

Smart sports shoes can include GPS to track the location of an athlete, heaters, and LEDs to emit light so that runners or cyclists can be seen at night.

Figure 2.5: Altra IQ Sports Shoes [4].

,

Smart bras are another smart garment usually used, made of conductive polymer coated fabrics. They can adapt to the breast movement, avoiding breast pain and sag.

Figure 2.6: Smart bra [5].

Most of the top-level football teams already use a GPS multi-sensor based technology approved by Fédération Internationale de Football Association (FIFA) on their players to track the multitude of statistics on speed, distance, heart rate, accelerations and dynamic stress loads [47].

Figure 2.7: A football player, using this technology during a football match [6].

,

In Portugal, around 60 thousand euros were spent in this technology for football teams from Portuguese league such as Benfica, Porto and Sporting [6].

2.1.5.3 Security and military

In mission-critical scenarios, the use of smart garments can bring several advantages.

These devices can provide continuous monitoring for military or firefighters that allows the measure of bio-signals indicators such as heart rate, stress, fatigue, respiration and, even, the presence of poisoning gases.

For instance, in Portugal, a project named VR2Market is being developed to measure firefighters' vital signs, hydration levels, stress, and fatigue. The VR2Market consist of an adhesive and a device placed in the firefighters' helmet capable not only to monitor firefight condition in case of emergencies but also the presence of toxic gases such as carbon monoxide.

The Institute for Systems and Computer Engineering, Technology and Science (INESC TEC) Porto is in charge of this project in partnership with the Telecommunication Institute, Institute of Electronics and Informatics Engineering of Aveiro (IEEA), the portuguese company Biodevices and the Robotics Institute Carnegie Mellon University [48].

The smart garments are capable of responding to these measurements in real-time, enhancing the user's productivity and safety.

The Defense and Public Safety sectors are already taking advantage of this technology to access position or health data. In addition, in some countries, cameras are being integrated into firefighters and military garments to record events [3].

2.1.5.4 Fashion Articles

For years, several smart garments have been developed for the fashion industry. As an example, we have the jacket developed in 2000 (Fig.2.8). This jacket can connect with the mobile phone and MP3 player. Furthermore, it includes built-in speakers, a microphone and a display.

Figure 2.8: ICD + Jacket [7].

,

There is another example developed by the MIT Media Lab - Levi's Musical Jean Jacket. It has a touch-responsive keyboard that allows the user to play music.

Figure 2.9: Levi's Musical Jean Jacket [7].

,

In New Zealand, another smart jacket was produced. Similarly to Levi's Musical Jean Jacket, it also has a keyboard. This keyboard is used to control the user's mobile phone (dial phone numbers, text messages, and play music) (see Fig.2.10).

Figure 2.10: Smart Jacket from New Zealand [7].

,

Smart clothes with light emitting textiles have been used in some fashion events such as catwalks (Fig.2.11).

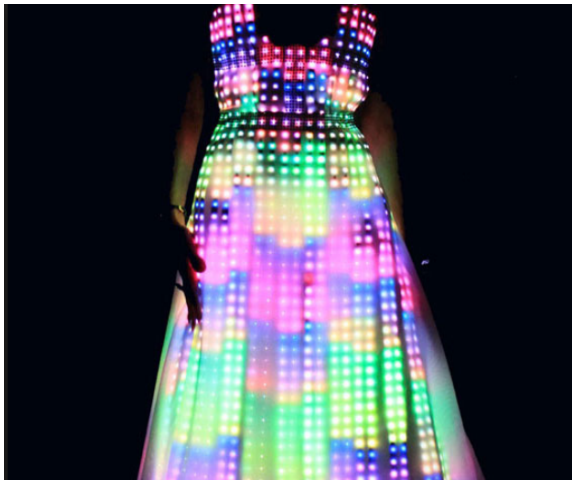

Figure 2.11: LED dress with wireless connection [1]

,

This technology can also be applied to interior design products such as sofa or pillows to control temperature, lighting, TV, etc (Fig.2.12 [49]).

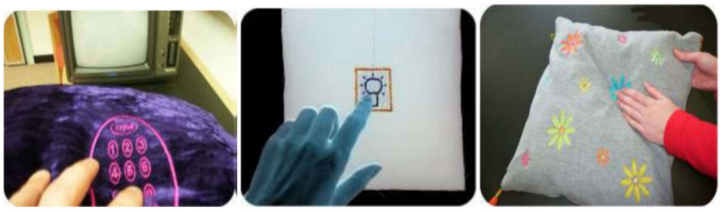

Figure 2.12: Interior design products with smart textiles [7].

,

2.1.6 Commercial Smart Garments Available

Throughout this chapter, several smart garments examples were presented. However, these examples were mainly prototypes (see subsection 2.1.1). Therefore, this subsection will focuses on some commercially available solutions for different applications.

Vital Jacket®, the first certified wearable medical device, was designed and developed at the University of Aveiro and licensed in 2009 by the company Biodevices, S.A. It consists of a t-shirt with embedded electronics capable of being used not only in hospitals or at home but also during daily activities of people with conditions that require frequent and continuous monitoring. This washable t-shirt includes ECG, 3-axis accelerometer and temperature sensors to record data. The

[1] https://www.thisiswhyimbroke.com/light-up-led-dress/ Accessed: 2019-01-10

data recorded can be transmitted via Bluetooth to another device or stored on SD memory card, for continuous or offline monitoring, respectively. [50, 9]

Currently, Biodevices SA provides five different versions of Vital Jacket (VJ) (Fig. 2.13): VJ Underwear (a comfortable and discreet version), VJ Sports (the perfect version for monitoring vital signs of the user during physical activities), VJ Baby (a bodysuit, instead of a T-shirt, for babies and toddlers), VJ Kids (for 3-8 year olds) and VJ Junior (for 8 to 14 year olds) [8].

(a) (b) (c)

(d) (e)

Figure 2.13: Different VJ versions available: (a) VJ Underwear, (b) VJ Sports, (c)VJ Baby, (d)VJ Kids and (e)VJ Junior Adapted from [8].

Fig. 2.14 shows two other smart garments capable of acquiring ECG signals with CE approval: nECG Textile from Nuubo® and Smartex Wearable Wellness System from Vivonoetics®..

Hexoskin® is another solution capable of acquiring ECG signals but, unlike the others, it does not present any type of certification [50]

All of these solutions also are capable of transmitting the acquired data for external devices which ensures real-time monitoring.

To measure vital signs Equivital System, Hexoskin Smart T-shirt may be use (Fig. 2.15) [9].

Equivital is a belt to be placed around the upper chest. It measures respiration effort using a strain gauge, two-lead ECG, 3-axis acceleration and skin temperature.

(a) (b)

Figure 2.14: Smart textile for ECG signal acquisition with CE approval:(a) nECG Textile from NuuboR® and (b) Smartex Wearable Wellness System from Vivonoetics®

(a) (b)

Figure 2.15: Smart garments to measure vital signs: (a) Equivital System and (b) Hexoskin Smart T-shirt [9].

Hexoskin smart consists of a t-shirt that measures breathing through magnetic sensors, one-lead ECG and 3-axis accelerometers.

Regarding sports applications, the APEX Athlete Series is a GPS performance tracker developed by STATSports. The GPS device is placed into the vest and can connect not only with mobile devices but also with different sensors via Bluetooth. The data can be directly sent to the STATSports app enabling real-time tracking.

STATSports is a company that provides player data to the most elite football teams such as Juventus, Liverpool, Manchester United, Manchester City, Paris Saint-Germain, etc. The data is analyzed to improve the player's performance and to detect possible injuries

Figure 2.16: APEX Athlete Series GPS performance tracker [10].

The prices for these solutions were not available in their companies' website, except for the Hexoskin Smart T-shirt (from € 151 to € 518) [51] and the APEX Athlete Series (€ 234.99) [10].

2.2 Market trends for wearable devicess

It is estimated that, in 2011, 14 million wearable devicess were sold based on an IMS Research [52]. The wearable devices coupled with the notable advances in smart textiles generated inflation in the general interest in this technology. In 2016, Fung Global Retail and Technology report noticed a significant increase of 18,4% to total 28.7 billion dollars in the wearable market between 2015 and 2016. Apple, Fitbit, and Xiaomi were identified as the main wearable companies and the smartwatch as the most sold device [53].

According to Forbes, the wearable market is expected to reach 34 billion dollars by 2020 [54].

Although it is impossible to predict with certainty if the wearable market will become more focused in smart textiles, the advantages they bring are clear and will be an influencing factor.

The current smart textile market was estimated at 100 million dollars per year. Some sources estimate this market to reach 5 billion dollars by 2023 [55].

2.3 Conclusion and challenges

Considering all the things discussed in this chapter, it is possible to conclude that the wearable market is experiencing fast growth over the last few years. They have several fields of application such as healthcare, sports, security, military and, even, in fashion.

In sports, wearables are mainly used to improve athletes' performance. Therefore, this approach that involves the application of wearables as a way to reduce resources waste in the sportswear industry has proofed to be an innovative concept.

To conclude, the integration of sensors into wearables is an extremely crucial step and presents a big challenge. It is essential to choose a material that assures the wearers' comfort. Smart textiles are always a good option when it comes to making this choice since they do not compromise the wearers' comfort. However, they can have lower results than a conventional sensor. The configuration of the electrical circuit that powers the sensor is another challenge. Regarding this topic, there are two main concerns. The first concern, related to the wearers' comfort, is the size of the sensor and its flexibility and the solution may involve flexible PCBs. The second, related to wearers security, is the circuit electrical isolation and impermeability. Logically, meeting all of these requirements is extremely challenging and complex.

Chapter 3

Strain sensors for textile integration

Although conventional strain gauges achieve high sensitivity, they are not stretchable enough to be implemented in wearable devices.

Due to the wearable market growth, the need for stretchable strain sensors capable of converting mechanical stimulus into electric signals has been increasing over the past few years [56].

Stretchable strain sensors can be used in several applications such as continuous health monitoring, sports performance enhancement and building of human-machine interfaces.

The most common stretchable strain sensors are of two types: capacitive and resistive. Among these two types, the resistive-type have been the focuses of several studies because it produces better results and has a simpler structure. Resistive-type sensors are usually obtained by embedding conductive materials inside polymers [11].

3.1 Operating Principle of strain sensors

Fig.3.1 illustrates the strain in a material that is given by the ratio between the change in length and the original material length (see Equation 3.1).

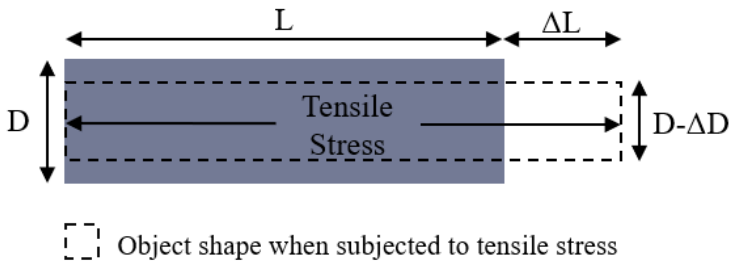

Figure 3.1: Strain in materials. Adapted from [11]

$$Strain\ (\varepsilon) = \frac{Change\ in\ length}{Original\ Length} = \frac{\Delta L}{L} \tag{3.1}$$

The strain can be negative - when the object is compressed - or positive - when the object is elongated.

Conventional strain gauges have a geometrical or piezoresistive effect on the basis of their operating principle.

In contrast to conventional strain gauges, the emerging resistive-type stretchable strain sensors operate mainly due to the disconnection, crack propagation mechanism and tunneling effect [56].

In this section, all these mechanisms and effects will be assessed in further detail.

3.1.1 Geometrical Effect

When materials are under tensile stress, they experience longitudinal and lateral strains, in opposite directions (Fig.3.2). Poisson's ratio (ν) is defined as the negative ratio between lateral strain and longitudinal strain. For stretchable strain sensors, the Poisson's ratio is approximately 0.5 [11].

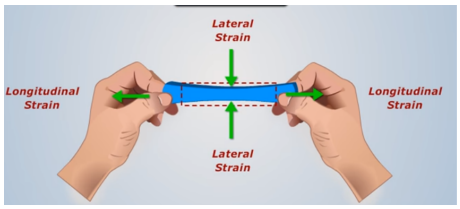

Figure 3.2: Longitudinal and lateral strains. Adapted from [12]

The resistance of a conductor is given by:

$$R = \rho \frac{L}{A} \tag{3.2}$$

where ρ is the electric resistivity (a specific property of the material that is related to its opposition to the flow of electric current), L is the length and A the cross-section area. Therefore, an increase in the length or a decrease in the cross-section area leads to an increase of the resistivity.

The initial capacitance of a material is determined using Equation 3.3.

$$C_0 = \varepsilon_0 \varepsilon_r \frac{l_0 w_0}{d_0} \tag{3.3}$$

where ε_0 and ε_r are the electric and dielectric constant of dielectric layer, respectively; l_0 is the initial length, w_0 the initial width and d_0 the initial thickness.

When the a capacitive-type strain sensor is stretched, length changes to $(1+\varepsilon)l_0$, the width to $(1-\nu_{electrode})w_0$ and the thickness to $(1-\nu_{dielectric})d_0$.

$$C = \frac{\varepsilon_0 \varepsilon_r (1-\nu_{electrode}) w_0}{(1-\nu_{dielectric}) d_0} = \varepsilon_0 \varepsilon_r \frac{(1+\varepsilon) l_0 w_0}{d_0} \tag{3.4}$$

Considering both Possion's ratios equal to 0.5, capacitance is given by $(1+\varepsilon)C_0$. Thus, there is a linear relashionship between the capacitance of a capacitive strain sensor and the applied strain.

However, this relationship is not valid when the value of the strain is too large because, in those cases, the Poisson's coefficients are not equal to 0.5 anymore.

3.1.2 Piezoresistive Effect

Piezoresistivity is the name given to the change in the resistance of some materials when they are under structural deformations. For metals and semiconductors, this change can be given by $\Delta R/R = (1+2\rho)\varepsilon + \Delta\rho/\rho$, where $(1+2\rho)\varepsilon$ is the geometric effect and the $\Delta\rho/\rho$ the fractional material resistivity change.

3.1.3 Disconnection Mechanism

A strain applied to a stretchable strain sensor results in disconnections in the conductive material. These disconnections block the electrical connection pathway and, therefore, the resistance of the material increases. These disconnections must be reversible since irreversible disconnections lead to permanent damage of the sensor and lower accuracy values.

3.1.4 Crack Propagation Mechanism

Cracks are created in locations with high stress and defects. These cracks will expand and propagate, increasing the resistance of the material and affecting its electrical conductivity as a result. Under strains lower than the material critical strain, the sensor is capable of recovering its initial state by closing the cracks.

3.1.5 Tunneling Effect

The principal effect in resistive-type polymer nanocomposite sensors is the disconnection mechanism. Nevertheless, for small distances between conductive nanomaterials and polymer matrix, electrons are able to move through a pathway through tunneling effect. The electrical tunneling resistance is given by:

$$R_{tunnel} = \frac{V}{AJ} = \frac{h^2 d}{Ae^2\sqrt{2m\lambda}} exp(\frac{4\pi d}{h}\sqrt{2m\lambda} \tag{3.5}$$

where V is the electrical potencial, J the density of tunneling current, A the cross-section area, h the Planck's constant, d the conductor and elastomer distance, m the mass of the electron and λ the height of energy elastomer barrier.

3.2 Performance evaluation

To analyze sensor performance it is important to consider some essential metrics such as the sensitivity, stretchability, linearity, hysteresis, response, and recovery time, overshooting and durability [56].

In addition to these metrics, it may be interesting to consider features like fabrication cost [11].

3.2.1 Sensitivity

The most commonly used metric in the analysis of strain sensor sensitivity is its gauge factor (GF). For resistive-type strain sensors, the GF is calculated by:

$$GF = \frac{\Delta R/R_0}{\varepsilon} \tag{3.6}$$

where $\Delta R/R_0$ is the fractional change in the resistance and the ε is the strain applied.

For capacitive-type strain sensors the GF is given by:

$$GF = \frac{\Delta C/C_0}{\varepsilon} \tag{3.7}$$

Since the capacitance can be approximated by $(1+\varepsilon)C_0$:

$$GF = \frac{\frac{(1+\varepsilon)C_0 - C_0}{C_0}}{\varepsilon} = 1 \tag{3.8}$$

This explains the low GF values obtained by capacitive-type strain sensor.

The low values of capacitive-type sensors in comparison to resistive-type can be observed in table **??** .

Conventional strain gauges composed of metal-foils or semiconductors presents really satisfactory GF values (2 to 5 and 100 to 1000, respectively[56]).

Stretchable resistive-type strain sensors can also achieve good results. Extremely high values of GF have been reported and they can also be consulted in **??**.

The highest value of GF found was 102351, for strains between 342% and 300% [57]. This value is much higher than GF values in conventional strain gauges.

3.2.2 Stretchability

Conventional strain gauges composed of metal or semiconductors have a really low stretchability ($\varepsilon \leq 5\%$). Therefore, they cannot be used in wearable devices.

Hence, several studies have been conducted regarding the need for stretchable strain sensor for wearable integration.

In contrast to the conventional strain gauge, emerging flexible strain sensors provide conformality and high stretchability ($\varepsilon > 50\%$).

Due mainly to the intensive research concerning this topic and the advances in nanomaterial technology, many strain sensors, providing high stretchability values, have been reported. Some examples of strain sensors with stretchability values higher than 250% can be found in [58, 57, 59, 60, 61, 16].

3.2.3 Linearity

Linearity is an essential feature of strain sensors. A linear material resistance or capacitance variation according to the applied strain makes the calibration simpler and provides better results.

Besides resulting in a more complex calibration process, nonlinearity creates a need for periodic recalibrations.

The nonlinearity can be calculated by:

$$Nonlinearity(\%) = max(\frac{y_{data} - y_{straightline}}{y_{model}}, \frac{y_{data} - y_{straightline}}{V_{es}}) \tag{3.9}$$

, where y_{data} is the output data and the $y_{straightline}$ is the straight line that best fits the model and, the V_{es} is the end scale value.

It is believed that nonlinearity is the result of heterogeneous changes in resistive-type sensor morphology upon stretching. This fact explains why many stretchable resistive-type strain sensors present lower linearity than conventional ones: stretchable sensors operate in much higher strain ranges and, therefore, endure more heterogeneous morphology changes.

To overcome this problem, most of the stretchable resistive-type sensors that were reported present different GF for different strain ranges [13, 57, 59, 62, 60, 63, 64]. Fig.3.3 shows the linear behaviour of a Mxene-based sensor. Five different regions of strain can be identified, each one with a specific GF.

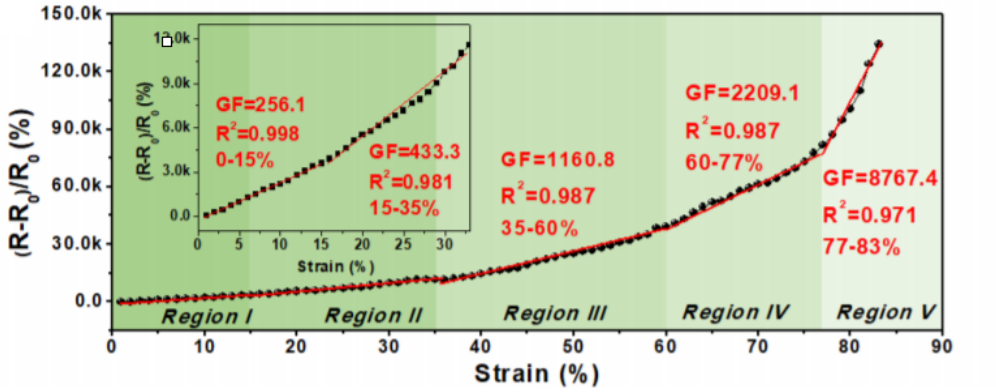

Figure 3.3: Linear behaviour of a MXene-based strain sensor [13]

The stretchable capacitive-type sensors usually have high linearity as shown by Fig.3.4.

However, as they present low sensitivity comparing to the resistive-type (as previous discussed in section 3.2.1), they are hardly used.

3.2.4 Hysteresis

The evaluation of the hysteresis of a strain sensor before its integration into the smart garment is essential, especially when the sensor is designed to be under dynamic loads. This happens, for example, in smart garments for motion continuous monitoring.

In a strain sensor, hysteresis is defined as the gap between stretching and releasing cycles and can be calculated by:

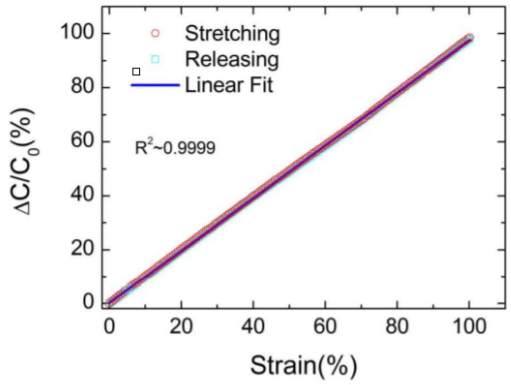

Figure 3.4: Behaviour of an capacitive soft strain sensor obtained by multicore-shell printing [14]

$$Hysteresis(\%) = \frac{h}{V_{es}} \times 100 \tag{3.10}$$

,where h is the maximum difference between the output values for the same input and is the end of scale value.

In contrast to capacitive-type strain sensors that are almost hysteresis-free, resistive-type sensors present a higher hysteresis [65]. This is reflected in figures 3.4 and 3.5.

In the capacitive-type (Fig.3.4) the stretching and releasing points fit the line with a coefficient of determination approximately equal to 1. For the resistive-type (Fig.3.2) there is a gap between the stretch and release curves.

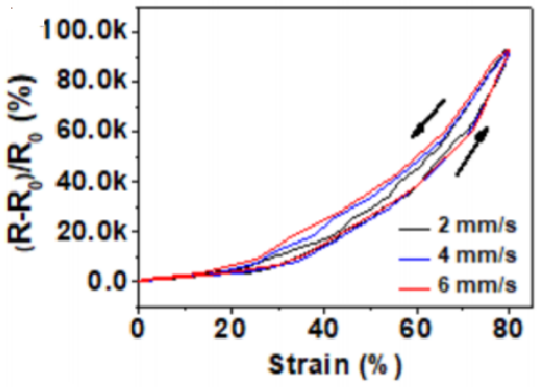

Figure 3.5: The behaviour of a MXene-based resistive-type stretchable strain sensors during stretch and release [13]

3.2.5 Recovery and Response Time

The response time of a strain sensor is the interval between an instantaneous variation of strain and the instant there is a change in the sensor output signal as a result of the previous strain variation.

The response of a strain sensor based on polymers has a delay due to polymers viscoelasticity.

Recovery time is the interval between the instant when the strain is removed and the instant the sensor reaches its steady state. Recovery time is an important feature to evaluate sensors designed to support dynamic loads.

A resistive-type sensor reported a response and a recovery time of 0.6s and 1.0s, respectively [66].

In [60], a resistive-type sensor with really low response time and recovery time (60.3ms and 60.4ms, respectively) was obtained.

Although resistive-type sensors present good response and recovery times, capacitive-types presents better results regarding these features. An example of this is a Carbon Nanotubes(CNTs)-Dragon-skin elastomer based capacitive-type strain sensor with response time about 40ms [16].

3.2.6 Overshooting

Overshoot behaviour of stretchable strain sensors was reported in resistive and capacitive-type sensors.

Fig.3.6 shows an example in which it was identified normalized peak values about 15% in a CNTs/polymers nanocomposite strain sensor due to overshooting [15]. Morteza Amjadi1 and Inkyu Park point out the polymers viscoelasticity as the main causing factor of the sensor overshoot behaviour. Other factors such as GFs of the material and strain range are present in [56].

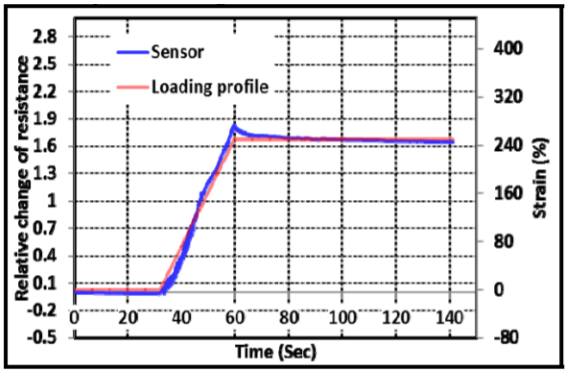

Figure 3.6: Overshoot behaviour of CNTs/polymers nanocomposite strain sensor [15]

3.2.7 Durability under dynamic loads

Durability under dynamic loads is the ability of the sensor to resist long-term stretching and releasing without compromising its performance.

This feature is very relevant for wearable strain sensors since they have to support high dynamic strains.

Although some studies reported degradation of the sensor when exposed to cyclic strains [67], others have shown good durability [16, 62, 57, 58].

Fig. 3.7 proves the high durability of a CNTs–Dragon-skin elastomer based capacitive-type sensor: Fig. 3.7a shows the relative changes in capacitance versus the number of cycles. The capacitance remained fairly constant as desired; Fig. 3.7b shows the relative change of capacitance over time. The overlapping between the baselines and the subsequent curves proves the high stability and reliability of the sensor.

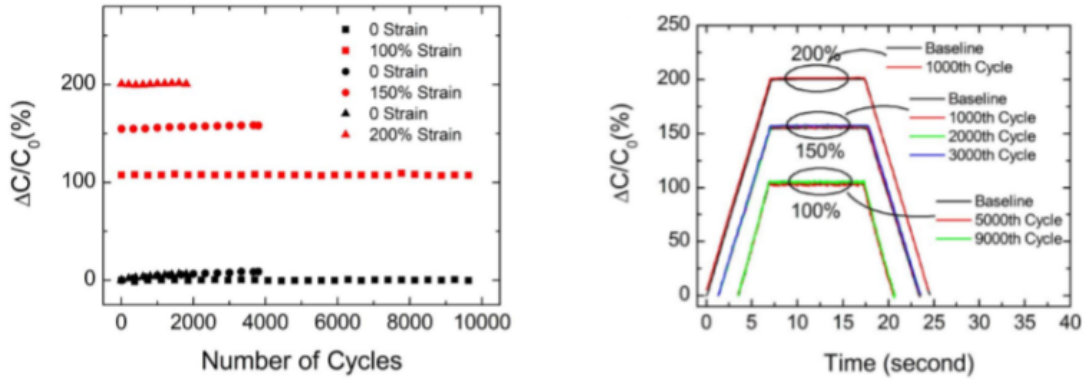

(a) (b)

Figure 3.7: Analysis of the durability of the sensor: (a) Capacitance relative variation over the number of cycles; (b) Capacitance relative variation over time [16].

3.3 Prototypes

Table 3.1 and 3.2 shows some of the reported prototypes with several different applications that range from epidermal sensors to motion monitoring [68].

These sensors are made of some materials such as graphene, carbon nanotubes and nanowires, etc.

3.4 Commercial Strain Sensors available

There are not many commercial strain sensors available and the ones available are in an embryonic state. Fig. 3.8 shows some of those examples.

Leap technology provides a wireless stretch sensor kit (see Fig. 3.8a). This kit includes two highly stretchable capacitive stretch sensors that are connected through cables to a wireless measurement electronics and it costs €550.00 [76]. This wireless measurement electronic can measure up to 4 sensors simultaneously. The capacitance of the stretch sensor changes from 1 at rest to 5 nF at full stretch in a non-linear way. The kit also includes a graphical user interface.

The Bend Sensor® is a resistive sensor (see Fig.3.8b [76]). Developed by Flexpoint, the sensor may be designed according to the application and connects to an electronic system that measures the bending or movement. The sensor sold with the kit costs €35.82 and €3.88 when sold separately.

Table 3.1: Resistive solutions and some of their characteristics

Resistive Sensor	**GF**	**Stretchability**	**Linearity**	**Reference**
MXene-based	256.1 (0-15%) 433.3 (15-35%) 1160.8 (35-60%) 2209.1 (60-77%) 8767.4 (77-83%)	83%	Linear in 5 regions	[13]
Silver Flake/Nanoparticle based	7.1	80%	Linear	[69]
Printable CNTs layers/ Polydimethylsiloxane composites based	35.75	45%	Linear	[70]
Graphene-silicone rubber composites based (2.3 wt%)	143 (0-35%)	480%	Linear	[58]
Graphene-silicone rubber composites based	76.7 (0- 75%)	480%	Linear	[58]
Graphene-silicone rubber composites based (4.0 wt%)	50.7 (0- 110%)	480%	Linear	[58]
Graphene-silicone rubber composites based (5.0 wt%)	30.3 (0-170%)	480%	Linear	[58]
Poly nanofibrils percolated in silicone elastomer of polydimethylsiloxane based	32	100%	Linear	[66]
Microstructured metal nanowire/elastomer based	81	150%	Linear	[71]
Conductive cotton fabric based	95.64 (0-231.19%) 2183.14 (231.19-342.3) 102350.91 (342.3-400%)	400%	Linear in 3 regions	[57]
Polydopamine encapsulated CNTs/elastic bands based	5.06 (0-250%) 28.06 (0-530%) 52.97 (530-780%) 129.20 (780-920%	920%	Linear in 4 regions	[59]
Sandwich structures of PEDOT:PSS and elastomer based	14 (0-5%) 26 (5-10%) 70 (10-20%) 110 (20-30%)	30%	Linear in 4 regions	[62]
Reduced graphene oxide sensing liquids based	2.5 (0.1-1%) 31.6 (390-400%)	400%	Linear in 2 regions	[60]
Ultra-violet/ozone cracked carbon nanotube/elastomer based	293.1 (0-20%) 1020.2 (0-20%) 343.0 (0-20%) 42.1 (0-100%)	100%	Linear in 4 regions	[60]
Graphene woven fabric based	70 (0-10%) 280 at 20%	50%	Linear region (0-10%) Nonlinear (10%-20%)	[64]

Table 3.2: Capacitive solutions and some of their characteristics

Capacitive Sensor	GF	Stretchability	Linearity	Reference
Silicone-textile composite based	1.25	150%	Linear	[72]
Metal deposition and laser rastering based	0.90	85%	Linear	[73]
Contact-transfer patterning of carbon nanotube forests based	1	450%	Linear	[61]
Silver nanowires based	0.7	50%	Linear	[74]
CNTs–Dragon-skin elastomer	0.97	300%	Linear	[16]
Percolating nanotube networks based	0.99	100%	Linear	[75]

(a) (b) (c)

(d) (e) (f)

Figure 3.8: Some of commercial strain sensors available found: (a)Leap Stretch Sensor, (b) Bend Sensor®, (c)BendShort v2.0 , (d) StrechSense^{TM}, (e) Spectrasymbol flex sensor, (f) Tinkersphere strain sensor

BendShort v2.0 is a bi-directional piezo-resistive bend sensor that measures the angle between the ends of the sensor and flex radius (see Fig.3.8c [77]). It costs € 36.05.

StrechSense^{TM} developed a highly stretchable capacitive stretch sensor that comprises a stretch fabric sensing element and a sensing board (see Fig.3.8d [78]). The sensor can be stretched up to 80 mm with almost linear behavior, has a sensitivity of 3.26 pF/mm and a base capacitance of 601 pF. The company also developed an app for iOs and Android in order to communicate with the sensor. Each kit containing ten sensors costs approximately € 1934.

Spectrasymbol resistive flex sensor resistance increases from 10k Ohm (flat state) to twice as high (bend state). a flex resistive sensor (see Fig.3.8e [79]). The Tinkersphere sells a resistive strain sensor (see Fig.3.8f [80]). Unlike most cases, the resistance of the sensor decreases with the strain (around 100K ohms to 40K ohms). The price of this solution was not available in the company' website.

3.5 Applications

Stretchable strain sensors can be used in health monitoring to record some motions related to the pulmonary respiratory function, arterial pulsation, cough, and swallow.

The information recorded may be important, for example, to evaluate the risk of suffocation against diseases and to detect some conditions such as dysphagia [62].

In sports, stretchable strain sensors can provide data essential to improve the athletes' performance or, even, to avoid lesions. They are capable of monitoring the motion of the wrist, pulse and the bending of the knee in some activities such as walking and running [13].

As strain sensors are able to detect human body motions, their application as human-machine interfaces would be worthwhile for the evolution of the artificial intelligence field [59].

3.6 Conclusion and challenges

All things considered, obtaining stretchable hysteresis-free strain sensors with high sensitivity and linearity is still a great challenge, mainly in biomedical applications that require highly sensitive and soft sensors.

Although resistive-type strain sensors with high sensitivity and stretchability have been widely reported, they can present a high degree of hysteresis and nonlinearity under high strains.

In contrast, capacitive-type sensors are nearly hysteresis-free and present high linearity. However, they have low values of sensitivity due to their theoretical limitations.

As many sensors reported coupled strain and pressure sensitivities [60, 74], it may be worthwhile trying to decouple them. In order to do so, there is a need for new materials and techniques.

Another interesting challenge is to include new features such as power, signal conditioning, and communication in the strain sensors [74]. However, this needs to be done without compromising the stretchability and size of the sensor to ensure its integration into wearable devices. This

is essential because, in wearable devices, such as smart garments, the wearers' comfort is a key pre-requisite.

Chapter 4

Strain sensor textile selection

4.1 Motivation

As already concluded in Chapter 3, developing stretchable hysteresis-free strain sensors, with high sensitivity and linearity is still a huge struggle. As it is intended to ingrate these sensors in wearables, other properties are required: for example, they have to be soft, stretchable enough to follow body movements and waterproof, since they will be exposed to adverse conditions, such as rain and athletes' perspiration.

As already seen before, resistive-type sensors usually provide better results and, thereby, CITEVE provided several resistive-type materials/textiles. Some electromechanical tests were performed to these materials/textiles to study the resistance variation as a function of the displacement. The goal was to select the material with the best behaviour.

4.2 Materials, test conditions and data pre-processing

For the tests, a material testing Instron machine, a NI-myDAQ with two analog input channels, a computer with LabVIEW 2018 installed, copper conductive tape and an acrylic plate were used (Fig. 4.1).

The Instron machine applies the strain to the textiles, the NI-myDAQ measures the voltage difference between the ends of the fabric as well as the voltage of the output signal from the Instron Machine. LabVIEW 2018 calculates the electrical resistance and records it in an excel file. The copper conductive tape ensures better electrical contact between the textile fabric and the eletrical circuit, and the acrylic plate guarantees a stable sample fixation.

For each type of fabric and test condition, electromechanical tests were conducted with three repetitions each. Fig. 4.2 shows the difference between each type of test condition.

The linear condition (see Fig. 4.2a) consists of a linear increase of the strain applied until the displacement of the fabric reaches 30 mm. The decrease of the strain applied is also linear.

In the drop condition (see Fig. 4.2b) , the process is similar to the linear condition. However, the strain does not decrease in a linear way- it ceases, resulting in an instantaneous drop.

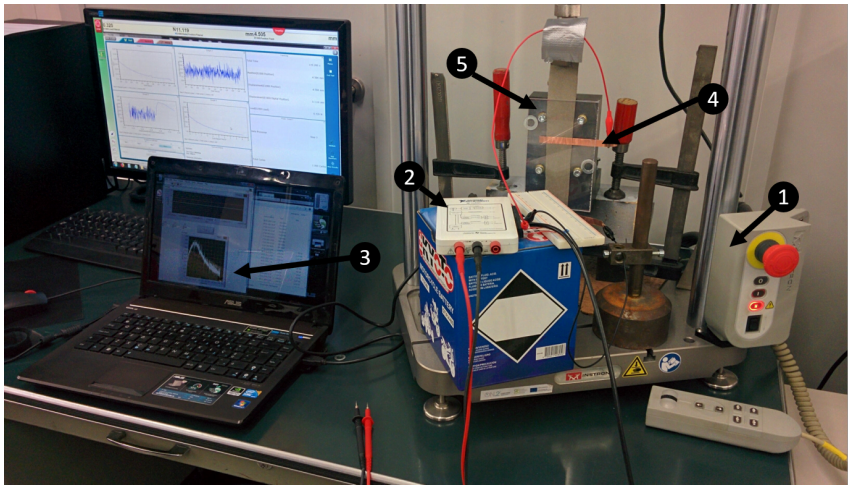

Figure 4.1: Materials for the testing of the textiles.

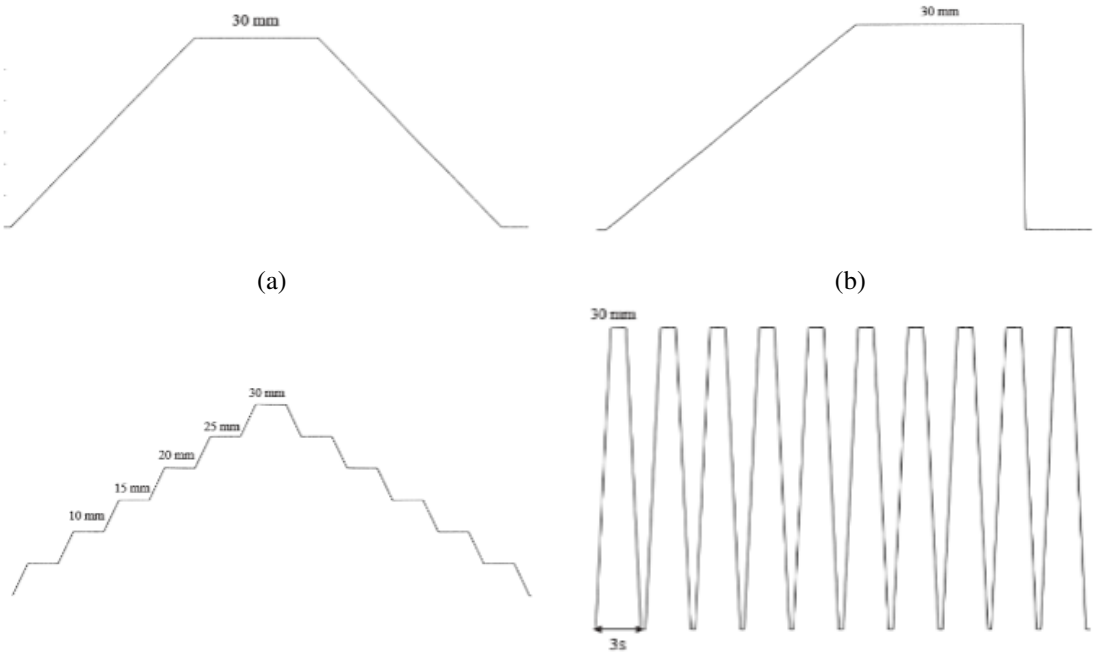

Figure 4.2: Test Conditions: (a) linear, (b) drop, (c) steps, (d) cyclic . Adapted from [17].

The steps condition (see Fig. 4.2c) is a result of an incremental increase of 5mm of textile fabric displacement until it reaches 30 mm of displacement and a following decrease with the same increment.

The cyclic condition (see Fig. 4.2d) consists of ten cycles of a strain increase until the 30mm of displacement of the fabric, followed by a decrease at the same rate. Each cycle has a 3-second duration.

The data needs to be pre-processed before performing data analysis.

The Instron machine output is a signal with a voltage proportional to the applied displacement. Therefore, the voltage values collect by the LabView needed to be converted into displacement.

Due to signal noise, a smoothing filter was required. Therefore, the MATLAB function "smoothdata" was used to apply a 0.5 seconds Gaussian filter (with a window size equals to 100 samples). Fig. 4.3 shows an example of an original and filtered signal of electrical resistance over time.

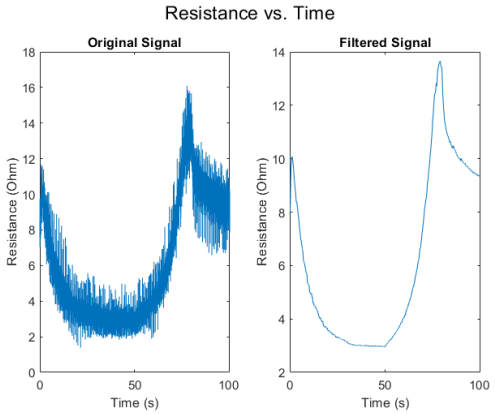

Figure 4.3: Example of an original and filtered signal of electrical resistance over the time.

For each linear test, to analyse hysteresis, the data was split into two parts (stretching and releasing data) using the derivative of the displacement signal (see Fig. 4.5a).

4.3 Textile tested

Table 4.1 summarizes the performed tests to the textiles provided by CITEVE. The tests consisted of five stages, each one with different purposes. In stage 1, the linear, drop and steps conditions were the conditions tested. From stage 2, it was decided to replace the steps condition by the cyclic in order to better simulate the actual conditions of strain sensor operational use- sports at which the movements are quick and cyclic as the case of cycling.

4.4 Analysis of the test data

In order to allow an easy and agile analysis, the data analyzed using MATLAB.

Table 4.1: Textiles and condition tested and the corresponding stage of testing.

Textile	Tested Conditions	Stage
P130+b [1]	linear, drop, steps	1
P180+b [2]		
Bi-elastic		
U-shaped P180+b (UP180+b) (w/ impermeable membrane 1mm)	linear, drop, cyclic	2
UP180+b (w/ impermeable membrane 5 mm)		
UP180+b (w/ impermeable membrane 1mm) wet		
UP180+b (w/ water repellent coating)	linear, drop, cyclic	3
UP180+b (w/ water repellent coating) wet		
Wire - 1st configuration (W1) [3]	linear, drop, cyclic	4
Carbon Conductive Paste (CCP) [4]		
Wire - 2nd configuration (W2)	linear, drop, cyclic	5
CCP		

[1] http://paolaguimerans.com/09_ShieldexTechniktexP130_18.12.12.pdf .
[2] https://statex.de/wp-content/uploads/2017/05/ShieldexTechniktexP180_02.10.13.pdf.
[3] https://www.adafruit.com/product/519.
[4] http://www.conductives.com/stretchable_smart_fabrics.php.

As tests were dynamic, the first step to determine tests uncertainty was to plot a histogram with 80 bins with all the data related to each textile (see Fig. 4.4 as an example).

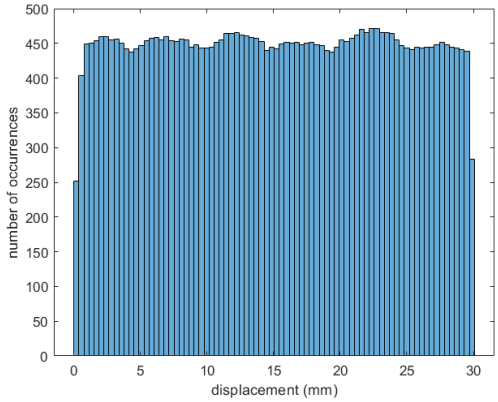

Figure 4.4: Histogram of displacement for P130+b.

The following equation allowed to compute the uncertainty for each bin with all the tests data related to each sensor:

$$Uncertainty_{bin} = \frac{\sigma_{bin}}{N_{bin}} \tag{4.1}$$

,where σ_{bin} is the standard deviation and N_{bin} the number of samples for each bin.

Finally, the uncertainty was given by the average of the bin uncertainties calculated in the previous step.

The sensitivity is given by the derivative of the straight line that best adjust to the textile response.

The first test was ignored for the calculation of the measures to evaluate the performance of the sensor and sensor calibration since as the sensor is in a steady-state, the values obtained are considerably different from the values of second and third test.

4.4.1 Stage 1

In the first phase, the goal was to determine the textile with the best behaviour among three textiles provided by CITEVE (P130+b, P180+b and Bi-elastic).

Fig. 4.5 shows the behaviour of each textile in linear tests.

It was decided to neglect the values for displacement lower than 5mm since there are several values with different displacements having the same resistance.

Table 4.2 shows the uncertainty, hysteresis, coefficient of determination, static sensitivity and nonlinearity for each textile.

Regarding the curve fitting, the data of both Bi-elastic and P180+b textiles can be successfully approximated since R^2 (coefficient of determination) values are very close to 1.

Despite the higher sensitivity of Bi-elastic, P180+b presents higher linearity.

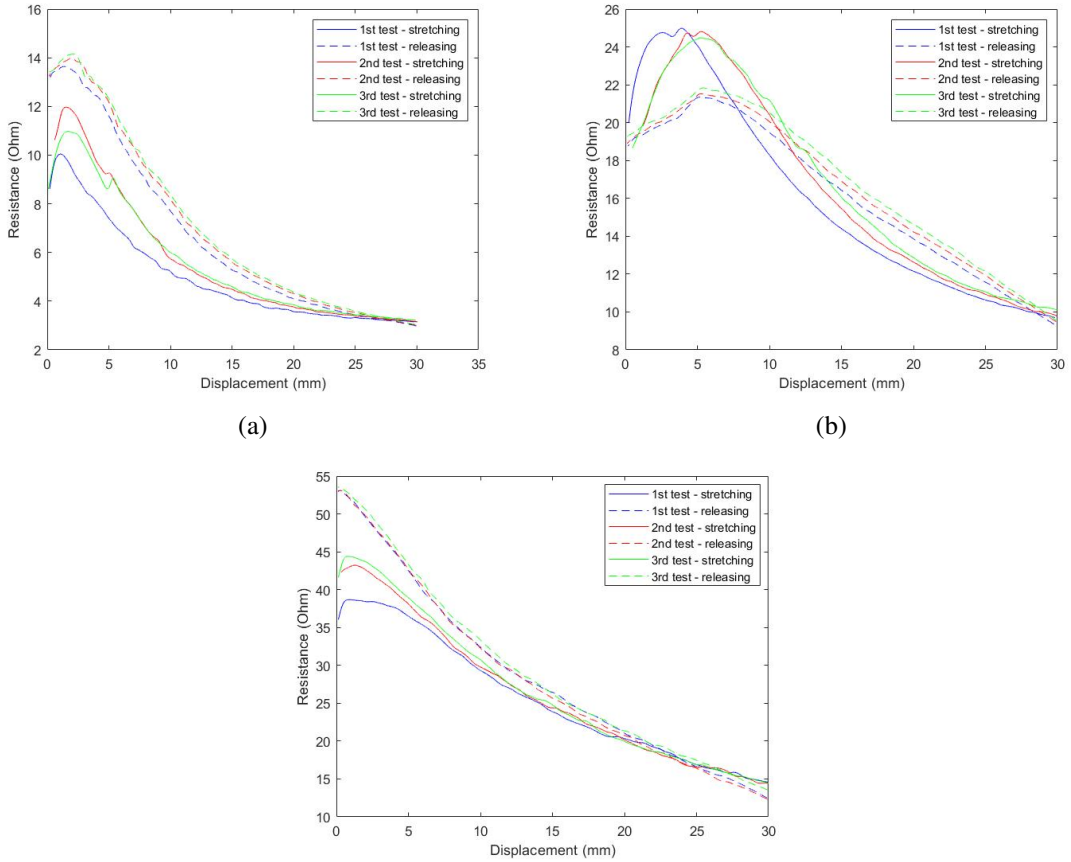

Figure 4.5: Resistance variation in linear test condition for: (a) P130+b, (b) P180+b, (c) Bi-elastic.

Table 4.2: Measures to evaluate textile performance (stage 1).

Textile	Uncertainty	Hysteresis (%)	Coefficient of determination	Static Sensitivity	Nonlinearity (%)
P130+b	0.002	34.78	0.88	-0.27	38.06
P180+b	0.003	19.83	0.95	-0.58	14.49
Bi-elastic	0.004	14.74	0.98	-1.02	20.27

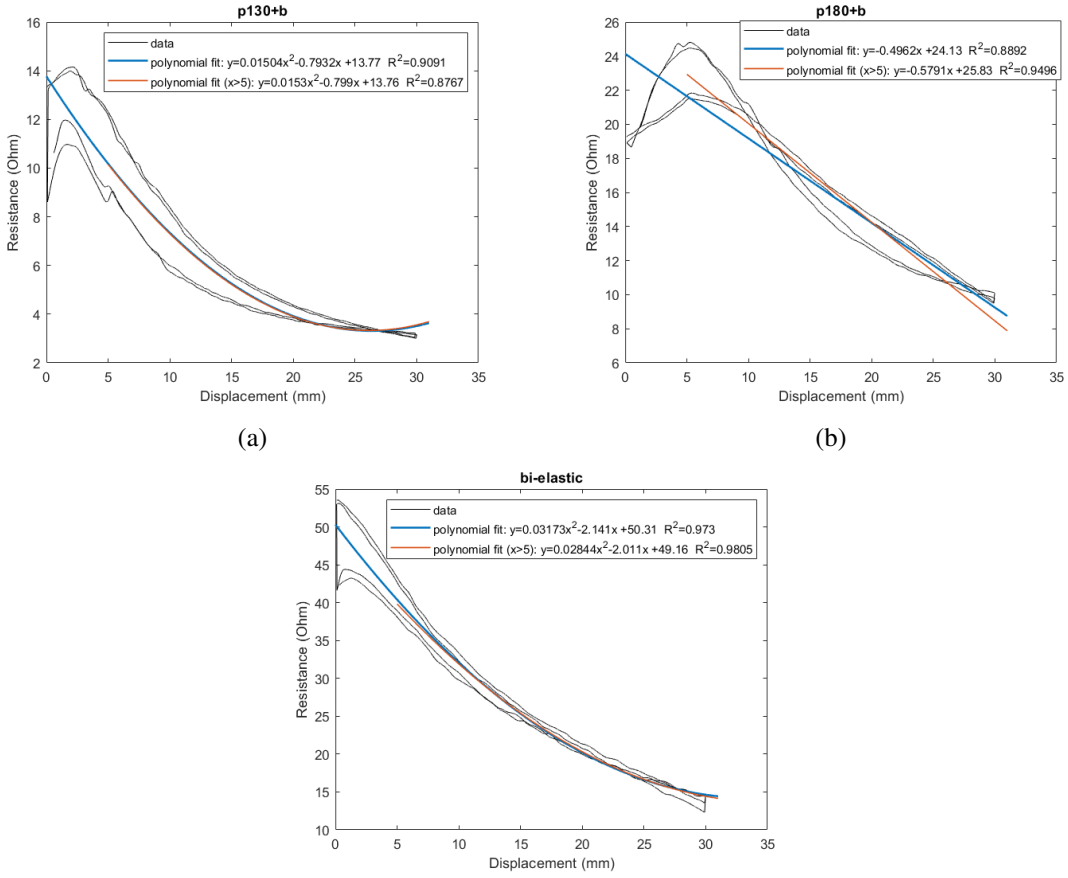

Figure 4.6: Calibration curves for: (a) P130+b, (b) P180+b, (c) Bi-elastic.

Besides that, Bi-elastic has a conductive rubber which is not desirable, whereas the P180+b presents a slight repellence effect which is advantageous. Therefore, considering the opinion of those involved in the project, it was decided to continue the work with P180+b.

4.4.2 Stage 2

The P180+b sample was change to an U-shaped configuration and then covered with an impermeable membrane to ensure that electrical resistance is not affected by water infiltration. Therefore, the stage 2 had the purpose of analyzing two UP180+b samples covered in both sides with an impermeable membrane. The textile structure is represented in Fig. 4.7b.

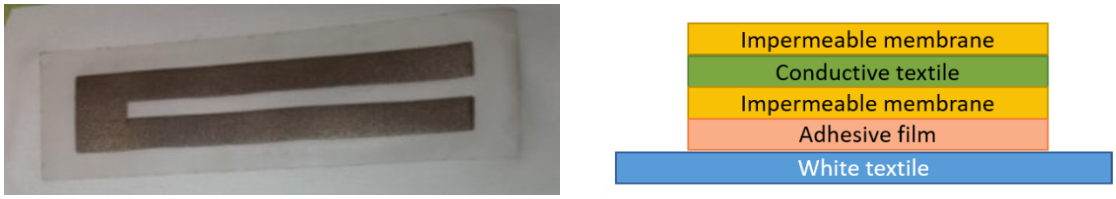

(a) (b)

Figure 4.7: UP180+b with impermeable membrane: (a) photo; (b) Structure representation.

The results for the UP180+b with impermeable membrane (1mm and 5mm) can be found in Fig. 4.8a and 4.8b, respectively. Comparing the obtained results for the P180+b with the impermeable membrane (1mm) and the results for P180+b obtain in stage 1, it is possible to conclude that the resistance in the steady-state increased due to the U-shaped configuration. However, the addition of the impermeable membrane had a significant negative impact, that becomes pretty evident in Fig. 4.8a: different values of displacement correspond to equal resistance values. The change in the P180+b behaviour may be due to the limitation in elasticity caused by the impermeable membrane (for a 3cm displacement of the white textile, the conductive textile suffered a 2mm elongation).

The significant differences between Fig. 4.8a and 4.8b may indicate that the textile with the 5mm membrane was damaged during the attempt to remove the membrane in the ends of the fabric (procedure needed to measure the resistance changes).

Fig. 4.8c shows the results obtained when the UP180+b with the 1mm impermeable membrane was slightly wet. Since the textile behaviour changes completely- resistance increases with the displacement, instead of decreasing as happened before -, it can be concluded that there is water infiltration. Therefore, the membrane does not fulfill its function and another solution is needed.

4.4.3 Stage 3

Since the impermeable membrane did not work as planned, another solution was designed: a UP180+b sample coated with a water repellent coating. This new solution presents the same

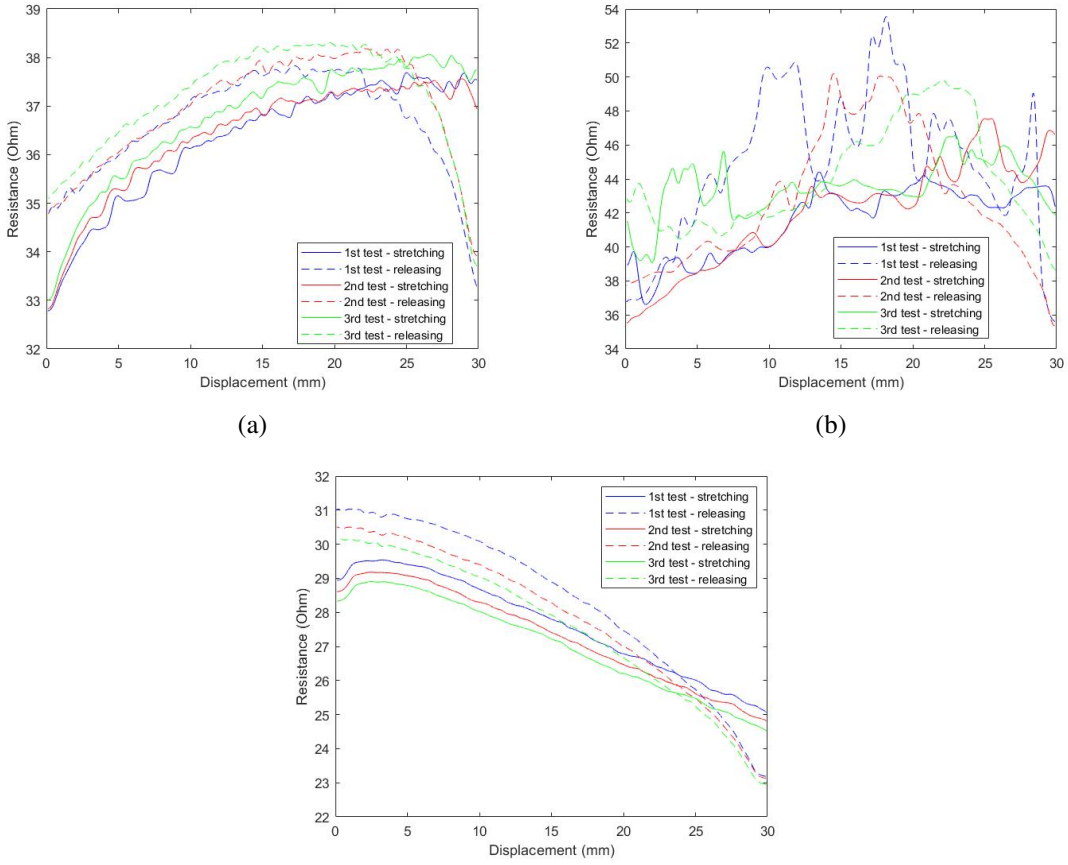

Figure 4.8: Resistance variation in linear test condition for UP180+b: (a) w/ 1 mm impermeable membrane , (b) w/ 5 mm impermeable membrane, (c) w/ 1mm impermeable membrane slightly wet.

structure of Fig. 4.7b. However, the impermeable membranes were replaced by a repellent coating in the top of the sample. The water repellent effect can be visualized in Fig. 4.9.

Figure 4.9: P180+b water repellent effect before its integration in the white textile.

Fig. 4.10a and 4.10b, respectively, show the behaviour of dry and slightly wet UP180+b coated with a water repellent coating.

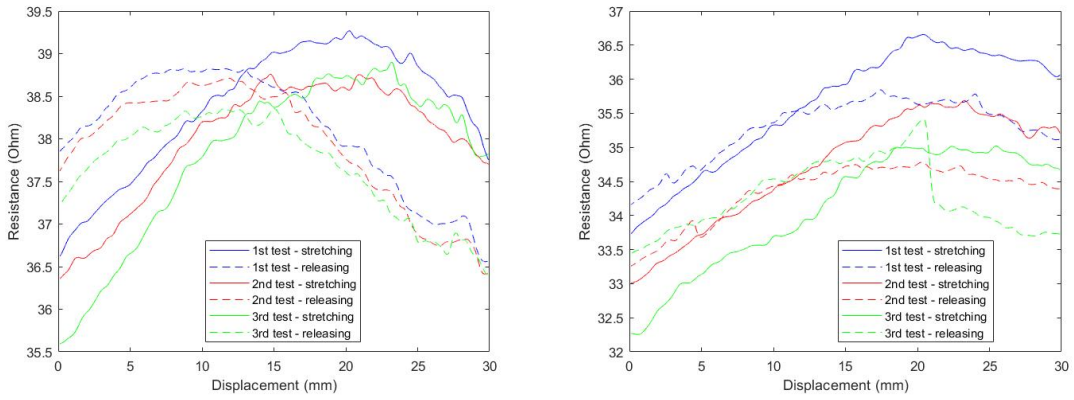

(a) (b)

Figure 4.10: Resistance variation in linear test condition for UP180+b with repellent coating: (a) dry , (b) slightly wet.

Comparing Fig. 4.10a and 4.10b with the behaviour of P180+b in stage 1, there are two things that can be concluded: the resistance in the steady state increases as a result of the U-shaped configuration. However, the behaviour of the textile becomes undesirable (several different values of displacement have the same resistance values).

Regarding the coating efficiency, although the behaviour of this textile doesn't alter completely when in contact with water, as happened in the last solution, it is noticeable a slight decrease in resistance over the tests which may be a result of water infiltration (Fig. 4.10b). Therefore, there was a need to explore other options.

4.4.4 Stage 4

For stage 4, another two possible solutions were provided for CITEVE: a W1 (see Fig. 4.11) and a CCP (see Fig. 4.12).

Figure 4.11: W1.

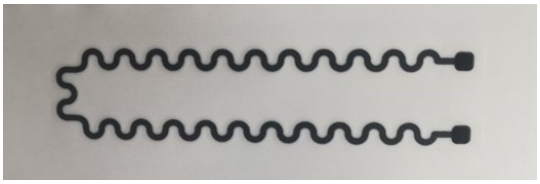

Figure 4.12: CCP.

The test data were analysed in terms of change in relative resistance change and absolute resistance. Fig. 4.13 shows the relative resistance change for the W1 in linear, drop and cyclic test conditions and Fig. 4.14 the calibration curve.

Table 4.3 shows the uncertainty, hysteresis, coefficient of determination, static sensitivity and nonlinearity also for the W1.

Table 4.3: Measures to evaluate textile performance (stage 4)

Textile	Uncertainty	Hysteresis (%)	Coefficient of determination	Static Sensitivity	Nonlinearity (%)
W1	0.002	10.62	0.98	0.57	80.00

Fig. 4.15 shows the results for the CCP in linear condition. The poor results may be due to a bad connection between the textile and the cooper conductive tape. The tests were repeated in the next stage.

4.4.5 Stage 5

For stage 5, the wire was placed in another configuration (see Fig. 4.16). The results obtained are shown in Fig. 4.17 and the calibration curve in Fig. 4.18.

Regarding the CCP, the results can be found in Fig. 4.19 and the calibration curve in Fig. 4.20.

Table 4.2 shows the uncertainty, hysteresis, coefficient of determination, static sensitivity, nonlinearity and response time for each textile.

Comparing the values from table 4.3 and 4.4, it was possible to conclude that the best configuration for the wire is the second. As the wire in the second configuration is embedded in the textile,

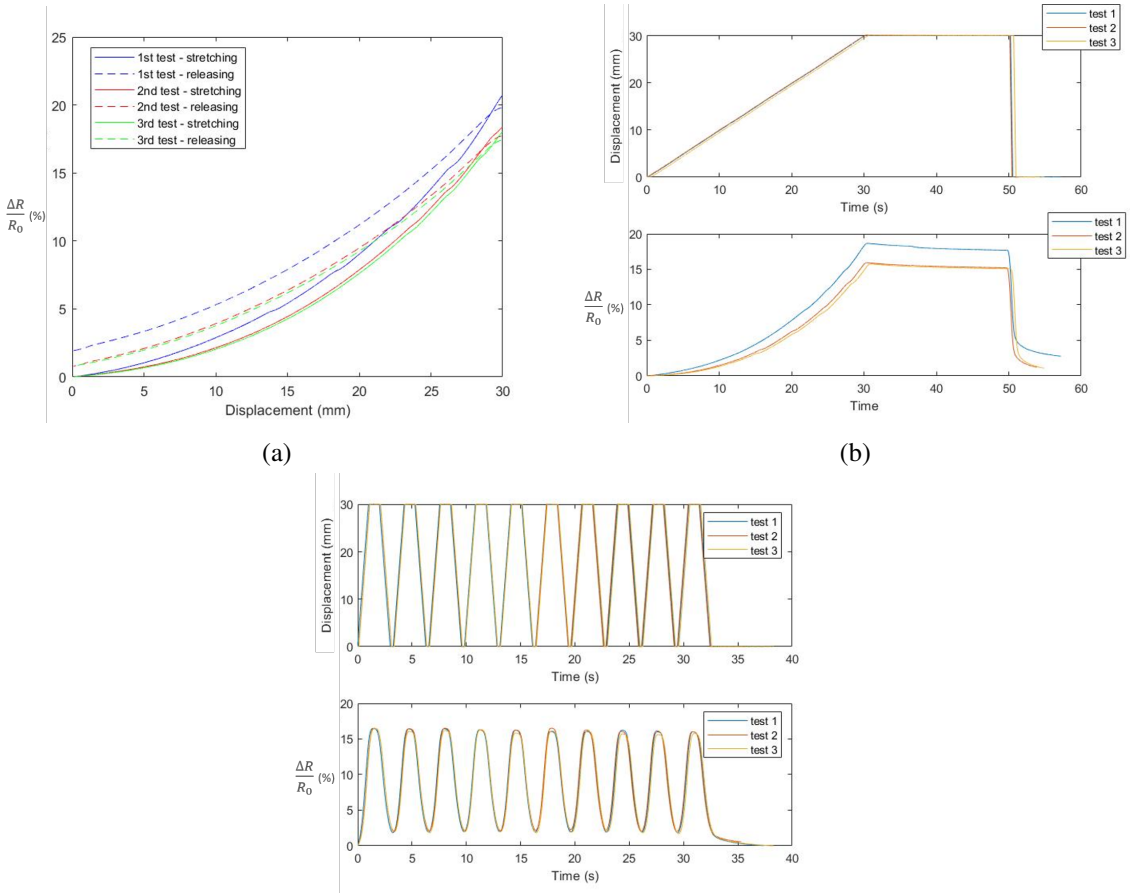

Figure 4.13: Relative resistance variation for W1 for: (a) linear , (b) drop and (c) cyclic condition.

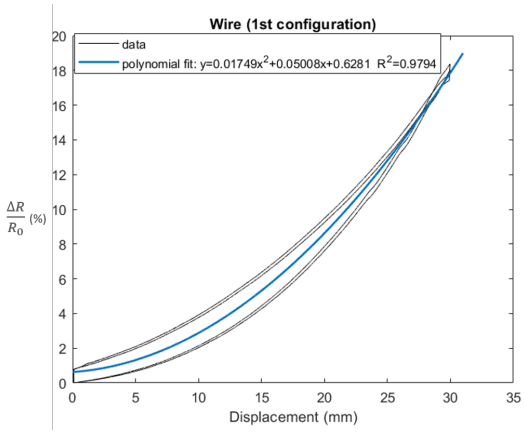

Figure 4.14: W1 calibration curve.

Table 4.4: Measures to evaluate textile performance (stage 5)

Textile	Uncertainty	Hysteresis (%)	Coefficient of determination	Static Sensitivity	Nonlinearity (%)	Response time (s)
W2	0.003	8.19	0.99	1.07	53.88	0.287
CCP	0.028	9.36	0.99	11.5	16.11	0.131

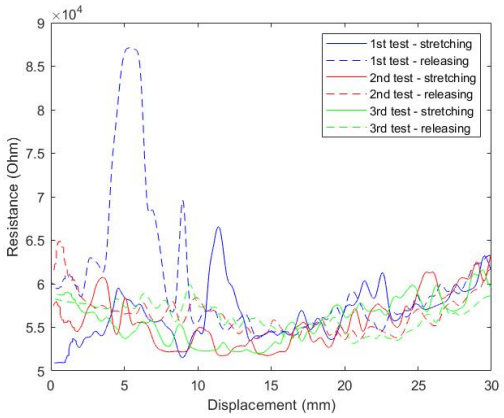

Figure 4.15: CCP resistance variation for linear test condition.

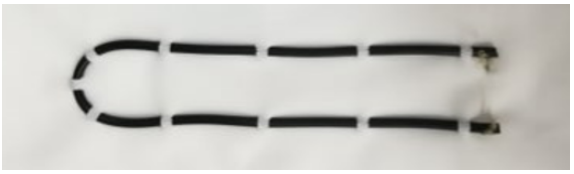

Figure 4.16: W2.

a displacement applied in the white textile results in a larger displacement of the wire which may explain the better results.

Although W2 results are quite satisfactory, the CCP seems to be the best solution with a higher coefficient of determination, sensitivity and nonlinearity, and lower response time. There is another advantage that can be observed in Fig. 4.21a and 4.21b: the CCP absolute resistance goes from approximately 100 kOhms to almost 800 kOhms that results in a range of approximately 700kOhm, whereas the W2 presents a lower range of 400 Ohms (1182.0 - 1586.8 Ohm). Regarding the wearers' comfort, the rubber of the wire can cause discomfort during practices, which makes the CCP the best solution.

The CCP is already impermeable which also constitute an advantage.

To compare this results with the existing prototypes, the displacement was converted into strain and the GF calculated. Fig 4.22 shows the relative resistance variation within the strain applied.

4.5 Conclusions

From all materials tested, the CCP is the one that presents the best behaviour. Although its GF is lower than some prototypes found in Table 3.1, there are more important variables to consider, such as linearity, hysteresis, response time and discomfort caused to the wearer. The CCP has linear behaviour, low hysteresis and low response time. In contrast to the majority of the prototypes found, that are encapsulated in rubber/silicone materials, the CCP is printed on the textile ensuring

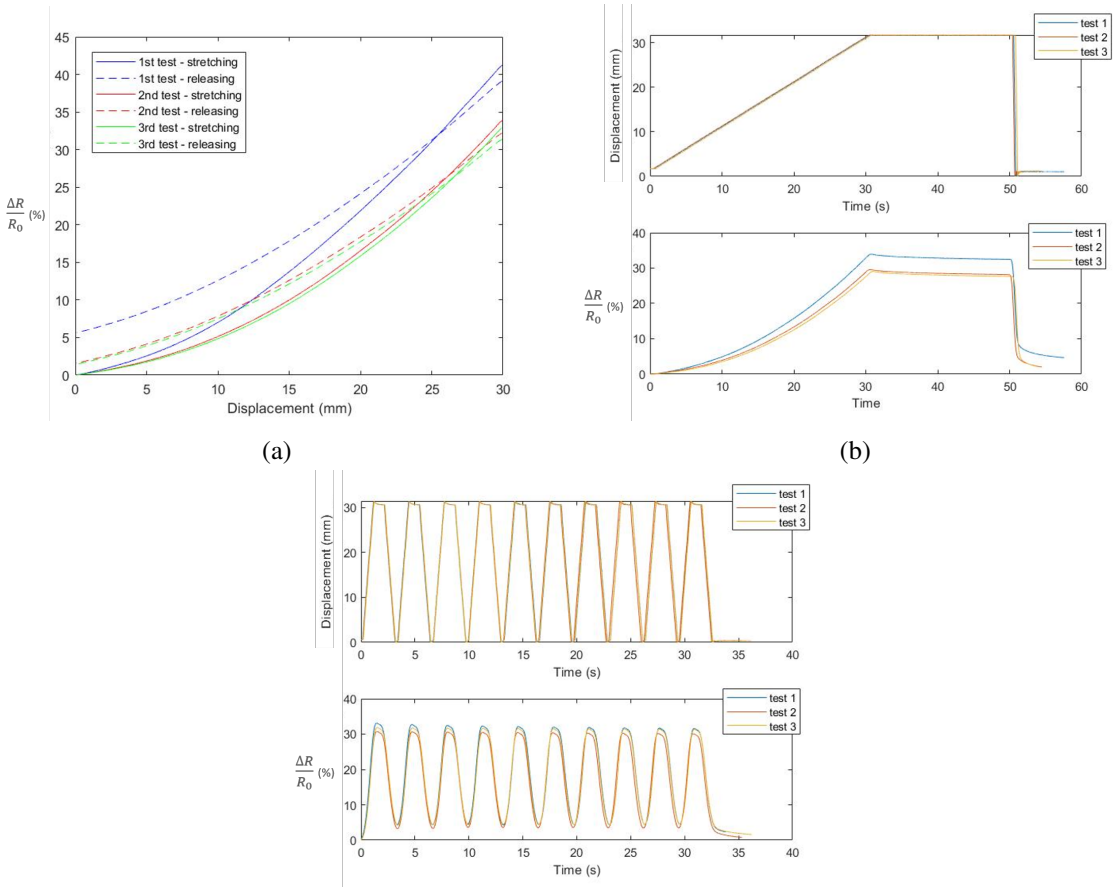

Figure 4.17: Relative resistance variation for W2 for: (a) linear , (b) drop and (c) cyclic condition.

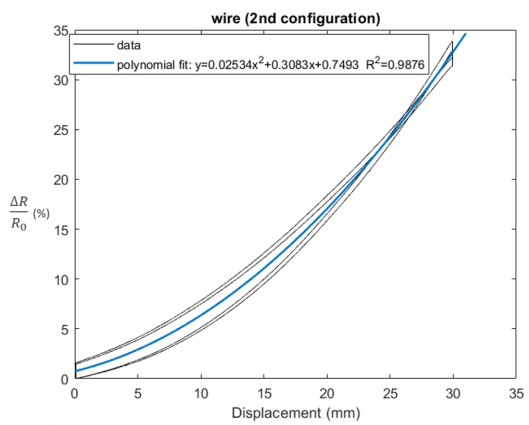

Figure 4.18: W2 calibration curve

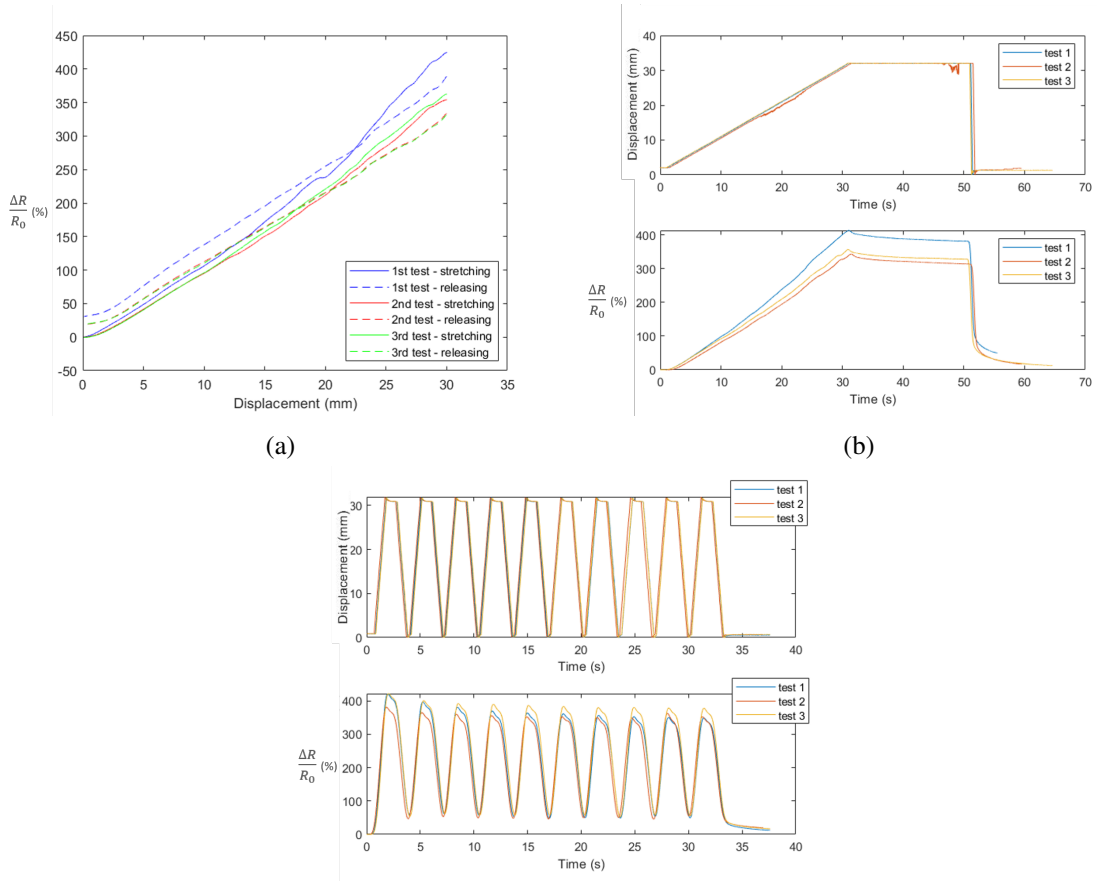

Figure 4.19: Relative resistance variation for CCP for: (a) linear , (b) drop and (c) cyclic condition.

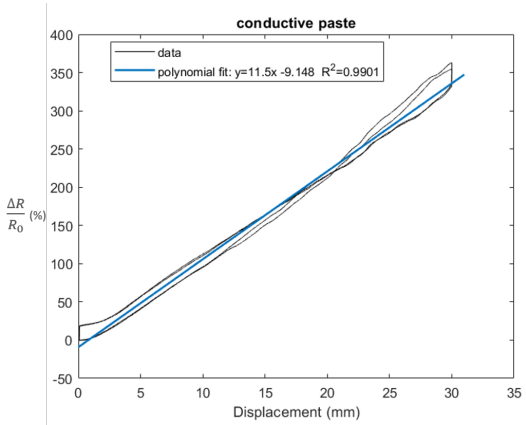

Figure 4.20: CCP calibration curve.

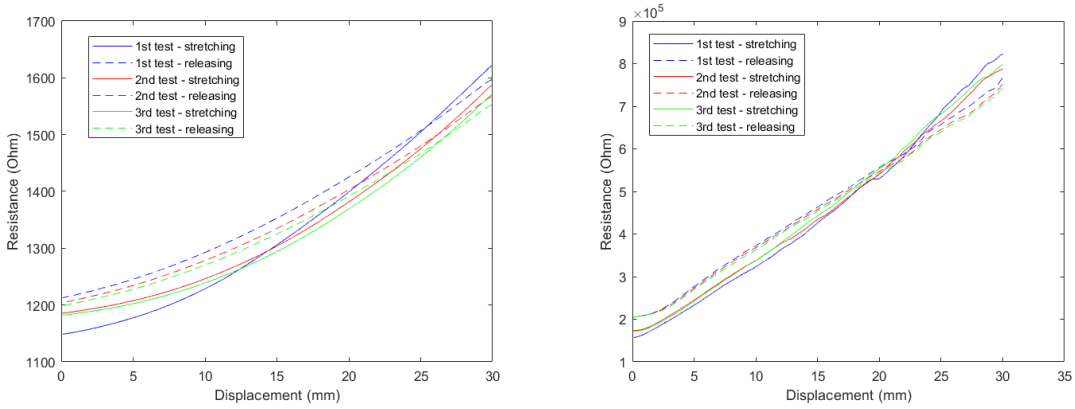

(a) (b)

Figure 4.21: Absolute resistance variation for: (a) W2 and (b) CCP.

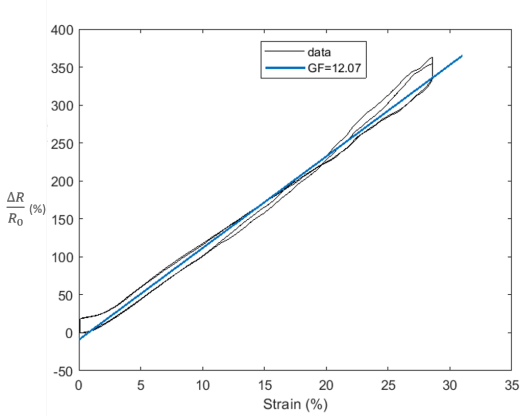

Figure 4.22: CCP relative resistance change vs strain graph

the wearers' comfort. These characteristics make this material a excellent solution for a strain sensor.

Chapter 5

Design of the sensor electronic circuit

5.1 Motivation

Fig. 5.1a shows the location of the different sensors and Fig. 5.1b a sportsman wearing the suit.

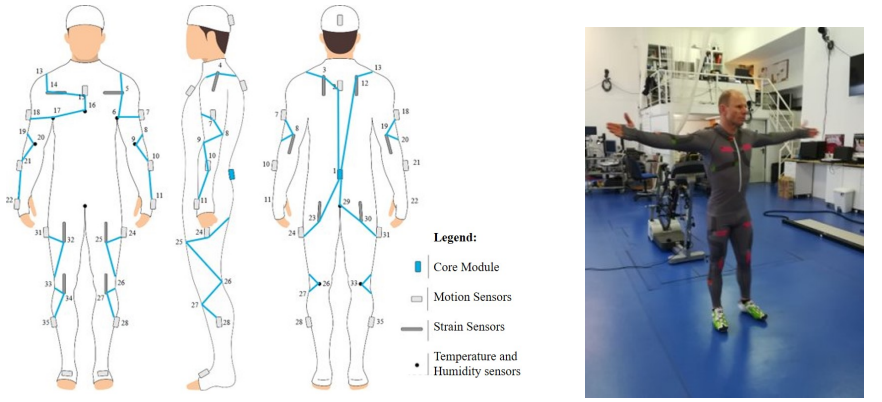

(a) (b)

Figure 5.1: wearable suit: (a) representation and (b) prototype.

The black lines in the suit (see Fig. 5.1b) correspond to the connections between the sensors and the core module. The core module sends the values measure by the sensors to the mobile application mentioned in section 1.2. Therefore, the values of displacement need to be sent from the sensor to the core module through I^2C [81]. For this purpose, an electronic circuit is needed.

5.2 Electronic circuits tested

The scheme of the first circuit tested can be found in Fig. 5.2.

The AD5933 is a high precision impedance converter, I^2C- compatible with a 12-bit ADC and a PGA with two possible gains (x1 and x5) [18].

Fig. 5.3 shows the AD5933 block overview. The frequency generator excites an unknown impedance resulting in a response signal. The response signal is sampled by the ADC and, after

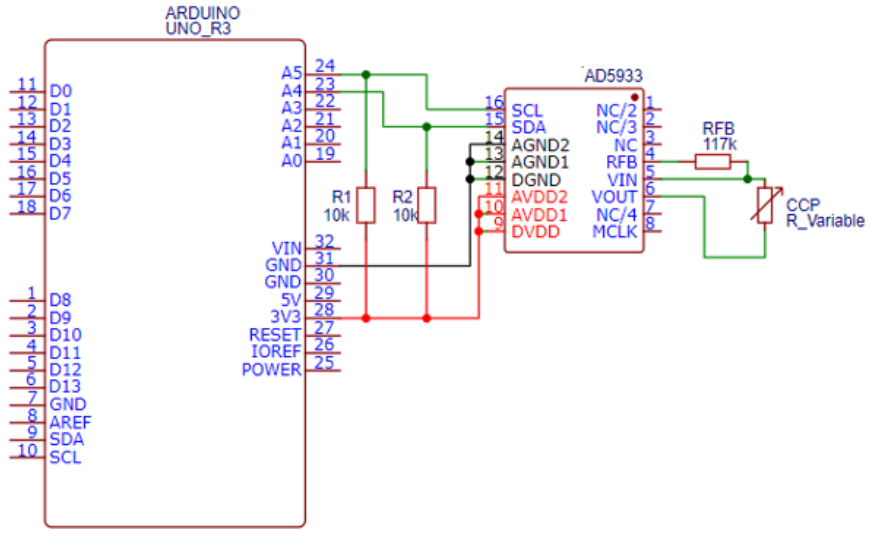

Figure 5.2: Scheme of the electronic circuit with AD5933 and Arduino UNO where CCP represents the conductive paste.

that, the DFT algorithm returns both real and imaginary values that enable the calculation of the phase and magnitude of the unknown impedance. As the sensor is resistive-type, the phase value is close to zero and the magnitude value corresponds to the sensor resistance.

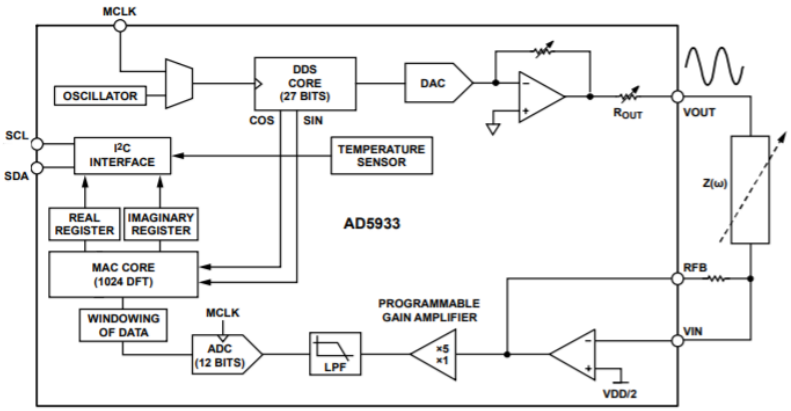

Figure 5.3: AD5933 block diagram [18].

The fact that the AD5933 has only one possible I^2C device address and the power consumption is too high (the typical power supply value during operation is 10 mA which corresponds to 140 mA for the 14 strain sensors in the wearable prototype) impossibilities its use on the sensor electronic circuit. Therefore, another solution using the ADS1115 was designed. This new solution requires a supply current in operation mode of 150μA, reducing the power consumption from 140 mA to 2.1 mA (about 67 times less).

The scheme of the second electronic circuit tested can be found in Fig. 5.4.

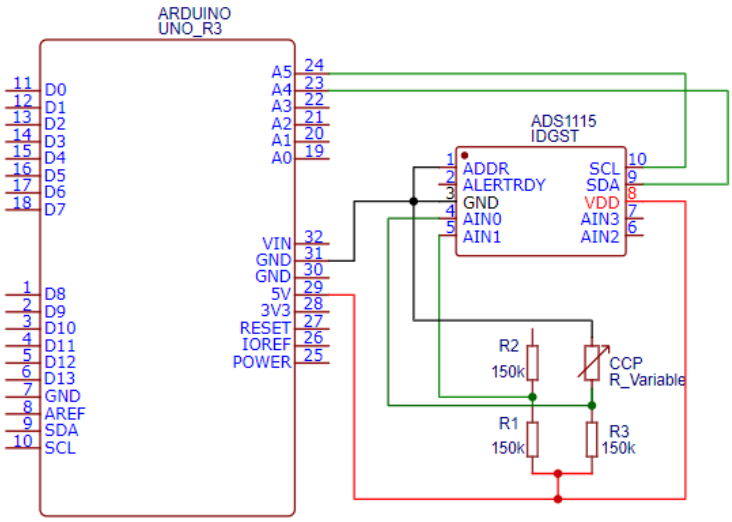

Figure 5.4: Scheme of the electronic circuit with ADS1115 and Arduino UNO where CCP represents the conductive paste.

ADS1115 is an ultra-small, I^{2}C- compatible and low-power, 16-bit ADC [19]. Fig. 5.5 shows the simplified block diagram of ADS1115.

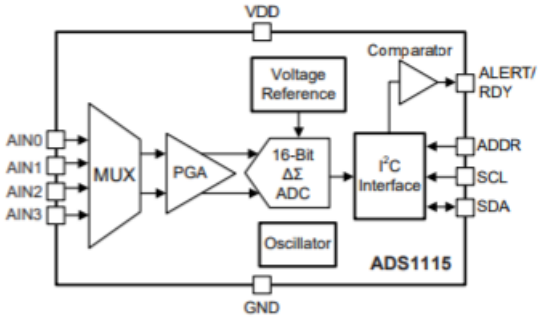

Figure 5.5: ADS1115 simplified block diagram [19].

The multiplexer provides two differential or four single-ended inputs. The PGA offers input ranges from $\pm$ 256 mV to $\pm$ 6.144 V, allowing precise large and small-signal measurements (with five gain ranges possible - 2/3, 1, 4, 8 or 16). The ADS1115 has four possible I^{2}C addresses and three modes (standard, fast and high-speed).

5.2.1 Results

The Arduino UNO was used as a master to receive the output values from the sensor using the I^{2}C protocol.

Regarding the communication with AD5933 circuit, modifications were made to the example "Z_LoggerComplex" from "AD5933_Library" Arduino library to convert the input impedance into displacement.

Concerning the communication with ADS1115, the example "differential" from "Adafruit_ADS1X15-master" Arduino library was modified to obtain the displacement values from the input voltage.

The sensor was manually stretched and released several times with different displacements for each circuit and the serial plotter tool was used to plot the results (see Fig. 5.6 and 5.7). The y-axis corresponds to the displacement (mm) and the x-axis to the number of samples (that is proportional to time). As expected, the sensor exhibits excellent behaviour for both circuits.

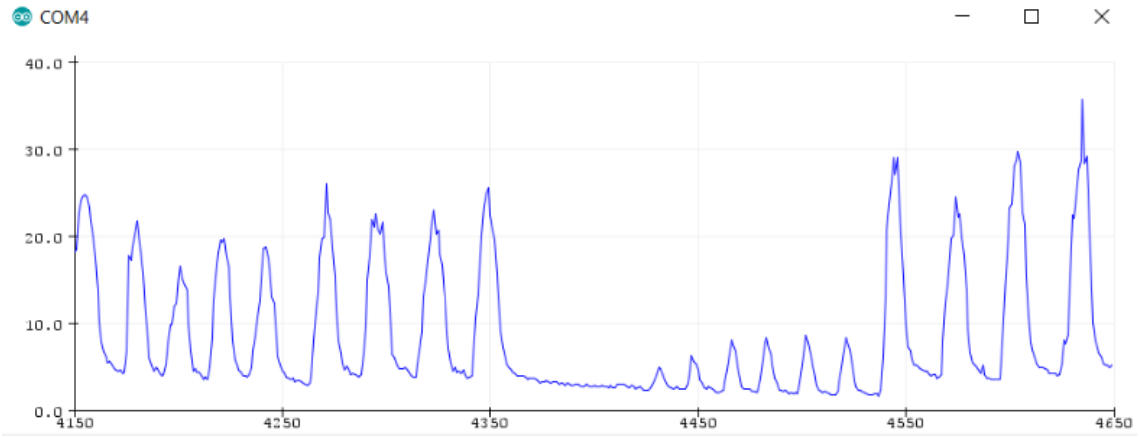

Figure 5.6: Results for the AD5933 circuity.

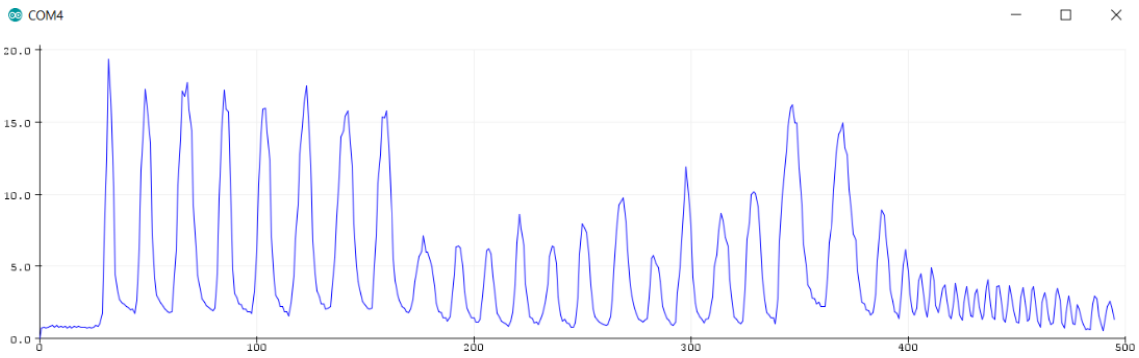

Figure 5.7: Results for the ADS1115 circuity.

5.3 Conclusions

The circuit chosen was the one with ADS1115 since it has significantly lower power consumption than the one with AD5933 and provides four different addresses for the I^2C communication.

Besides, the ADS1115 has higher resolution and more gain ranges possible.

The next step is to design a similar circuit into a flexible PCBs. After that, it is necessary to glue the PCBs in the predetermined regions and connect them properly to the wearable prototype wires. It is very important to ensure a good connection, since poor connection results in noise. For example, the low noise, visible mainly in Fig. 5.6, is due to the weak connection between the sensor and the breadboard.

Chapter 6

TexSense web application

6.1 Motivation

The main goal is to use the developed sensor in a wearable suit alongside other sensors. However, it may be interesting to use the sensor individually for some applications. In this case, there are some problems associated with its usability.

Arduino Serial Plotter allows users to see the displacement measured by the sensor in real-time. However, to be able to do that, users must download, install and learn how to use Arduino tools. These tasks may be difficult for some users and act as a limiting factor when it comes to using the sensor. Also, the fact that Arduino does not allow to save and view the data from older measurements in an organized and clear manner presents a significant problem.

Web apps do not require installation and are always updated. As users only need to deal with user interfaces and the rest is handled in the background, web apps are also highly intuitive and easy to use. Another advantage of web apps is related to data storage. Since they can connect with clouds, it is possible to save a large amount of information.

Therefore, to overcome the issues mentioned above and taking into account all the web apps advantages, it was decided to develop a web app.

6.2 Actors an Use-Cases

The starting point for building an app is to establish the actors and use cases of the system. Concerning the actors, in TexSense web app, three actors may be identified: non-authenticated user authenticated user and administrator. Regarding the use-cases, the non-authenticated user must be able to:

1. Login, register and access the about page of the app.

The authenticated user must be able to:

1. Change his profile information;

2. View the graphs of the displacement in real-time (with 4 sensors connected at maximum);
3. Add notes to each measurement in real-time;
4. Store and view all the stored information related to the performed measurements;
5. Search for measurements by title;
6. Report problems, see the administrator answer to those problems and be able to reply;
7. Mark a problem as solved;
8. Receive notifications when there is a reply to their report.

The administrator should be able to:

1. Receive a notification if a report is created or if there is a reply to their answer;
2. See the reports organized by categories (solved, answered but not solved and not solved);
3. Search for reports by title;
4. Maintain the proper functioning of the web app (being able to delete users or content that he considers inappropriate).

6.3 Database design

The database design was composed by two-stages: the Entity-Relationship diagram design and its mapping into a Relational Model.

Fig. 6.1 shows the Entity-Relationship Diagram (ERD) for the TexSense web app. An ERD is a type of structural diagram, used in database design, that allows the identification of the data to be saved, as well as the rules to be implemented. Entities, attributes and relationships (represented by Fig. 6.2) are the main components of an ERD. Entities are elements to be stored in the database and can be physical objects, such as users, or concepts, such as reports. Attributes are entities properties, and relationships are associations between two or more entities.

Cardinality constraint expresses the maximum number of entities that can be associated with another entity in a relationship. All relationships presented in the ERD of Fig. 6.1 have one-to-many cardinality constraints. For example, in the relationship between User and Report, one-to-many cardinality says that one user can create many reports, but one report can only be created by one user.

In contrast to cardinality constraint, participation constraint expresses the minimum number of entities that can be associated with another entity in a relationship. For instance, one user may not create reports (optional participation) but a report must generate at least one notification (total participation).

Detailed information regarding ER diagrams can be found in [82].

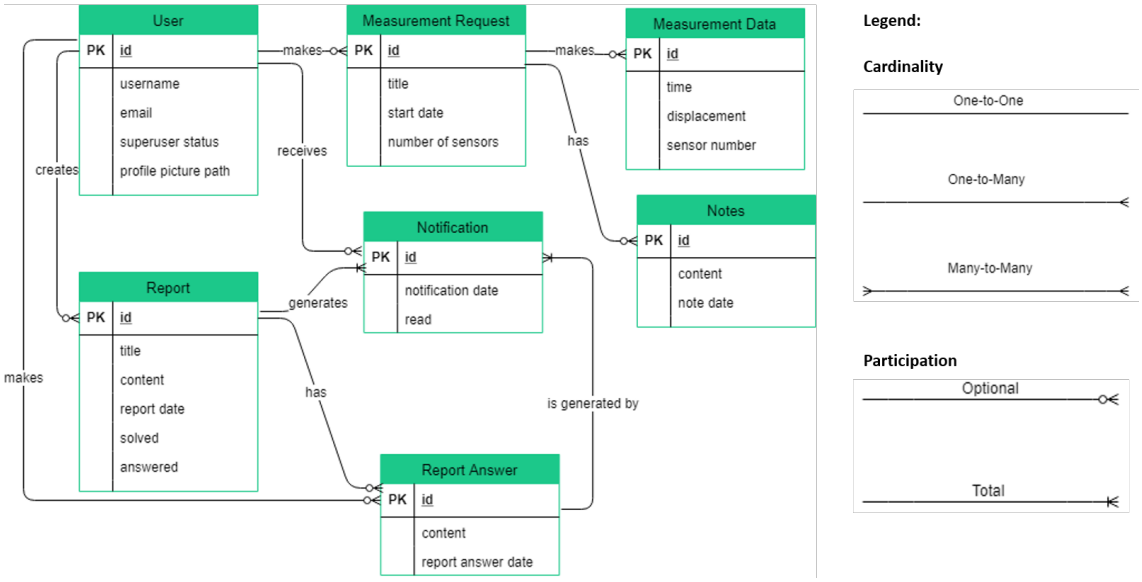

Figure 6.1: Entity-Relationship diagram of TexSense web app.

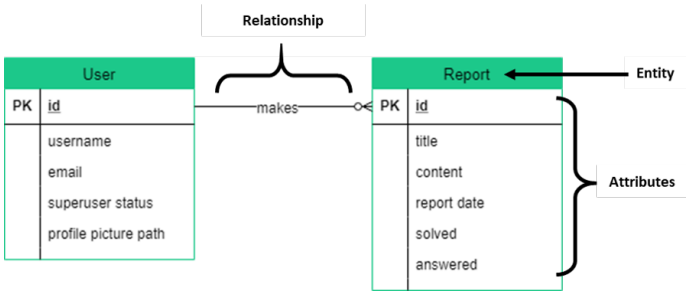

Figure 6.2: ERD partial diagram of TexSense web app.

The ERD in Fig. 6.1 was then mapped into the Relational Model presented in table 6.1, since Relational Model is the most used model for databases mainly due to its simplicity, easiness of data retrieval and flexibility (it is easy to add/remove and modify the attributes to meet the requirements of application). The rules to obtain a proper Relation Model from an ERD are presented in [83], as well as a detailed explanation regarding relations and constraints.

Table 6.1: TexSense web app Relational Model obtained through the mapping of the ER diagram.

Relation Reference	Relation Notation
R01	User(id, username **NN UK** , email **NN**, superuser_status **DF** False, profile_picture_path)
R02	MeasurementRequest(id, title **NN**, start_date **DF** current_timestamp, #user_id–>User **NN**)
R03	MeasurementData(id, time **NN**, displacement **NN**, sensor number **NN**, #measurement_request_id–>MeasurementRequest**NN**)
R04	Note (id, content **NN**, note date **DF** current_timestamp, #measurement_request_id–>MeasurementRequest **NN**)
R05	Report (id, title **NN**, content **NN**, report_date **DF** current_timestamp, solved **DF** False, answered **DF** False, #id_user–>User **NN**)
R06	ReportAnswer(id, content **NN**, answer_date **DF**, #report_id–>Report **NN**, #user_id–>User **NN**)
R07	Notification(id, #reportAnswer_id–>ReportAnswer, #report_id–>Report, #user_id–>User **NN**)

The relation reference is used to refer to a given relation throughout this section. For instance, R01 stands for User Relation. The notation of a relation is:

Relation (primary key, attribute 1, attribute 2, ..., attribute n, #foreign key –> Referenced Relation).

A relation must always have a primary key but does not always require a foreign key as is the case of R01. NN (not null), UK (unique) and DF (default) are some of the constraints. To understand the meaning of NN and UK constraints, let's look at the username attribute in R01. The NN and UK constrains for the username indicate username cannot be left empty and must be different from the existing usernames when a user is created/updated. Now, let's focuses on the R02 in order to try to understand the DF constraint. The DF constraint for the "start_date" means that if a user makes a Measurement Request and the "start_date" is left empty it will be filled automatically with the current date and time.

6.4 Prototype Development

TexSense web app was developed with Django. Django is a web framework that provides a standard easy way to develop websites. In addition to making the process of development extremely fast, reassuring security and being incredibly scalable and versatile, Django is also free, open and

a high-level Python Web Framework. By default Django creates a SQLite database - a lightweight relational database included with Python distribution [1].

Regarding the front-end, the user interfaces were created using HTML, Bootstrap, CSS, and Javascript to obtain highly responsive and user-friendly interfaces.

6.5 Demonstration of Prototype features

The features of the web app result from the implementation of the Use-Cases discussed in section 6.2. Some of these features are demonstrated in the Prototype demonstration video (link in the footnote) [2]. In this demonstration, the Arduino is used to simulate the data from 4 sensors by generating random values, since there is only one sensor available.

Since the video may become unavailable, screenshots that show the user interfaces (UIs) were added to this chapter.

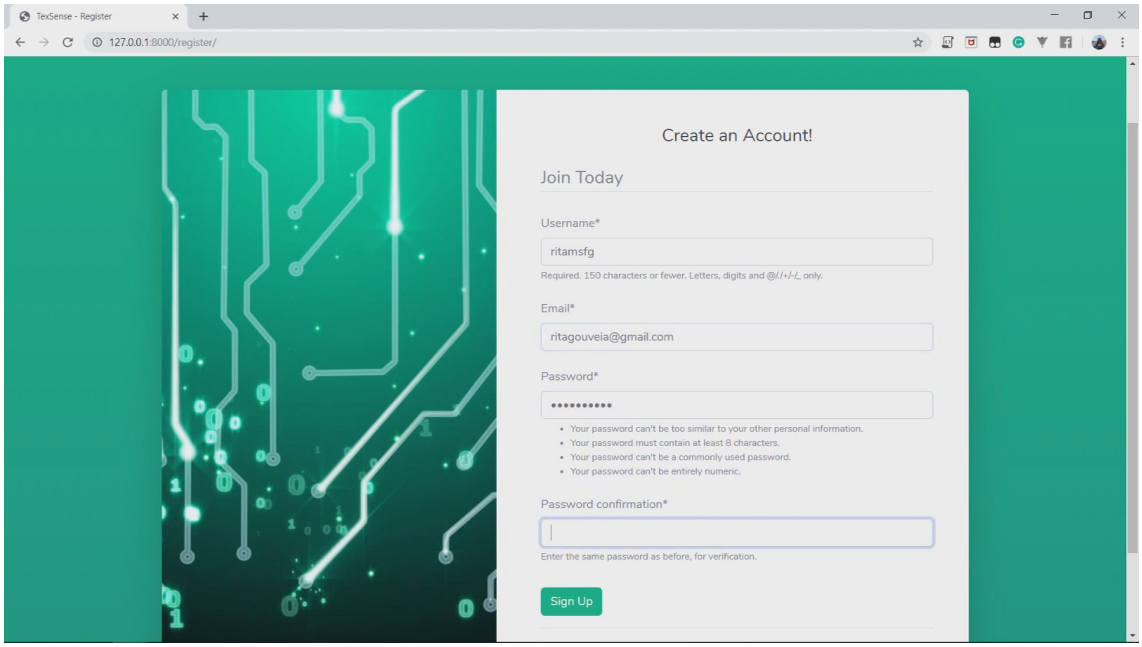

Figure 6.3: Register UI.

6.6 Conclusions

All things considered, it was developed a fully functional prototype that complements the developed sensor, providing a better experience to the users. This app, combined with Arduino, can read sensors output and store the data related to each measurement. The users are now able to see

[1] More information at: https://www.djangoproject.com/

[2] See Prototype demonstration video at: https://www.youtube.com/watch?v=jhz1p9EnNbY&feature=youtu.be

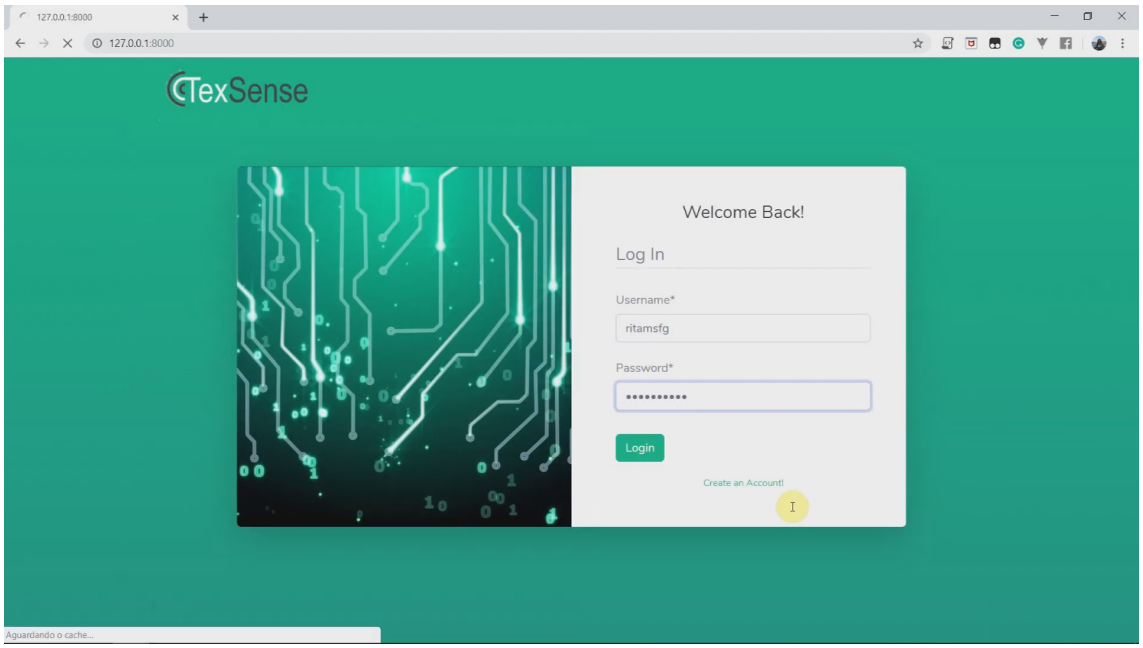

Figure 6.4: Login UI.

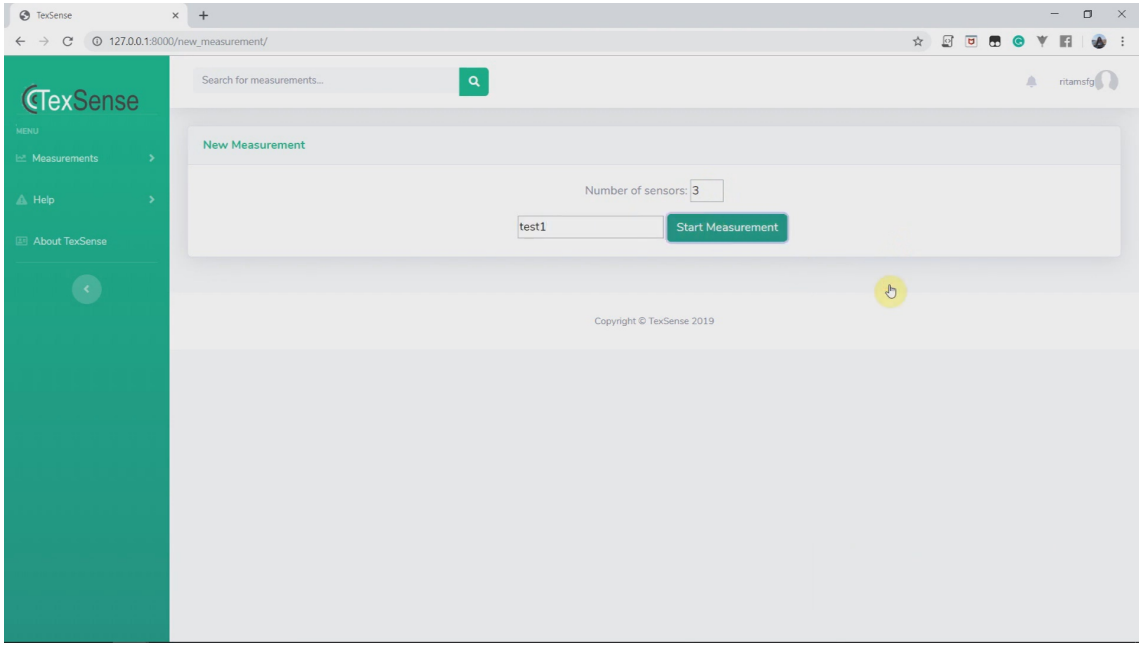

Figure 6.5: Create Measurement UI.

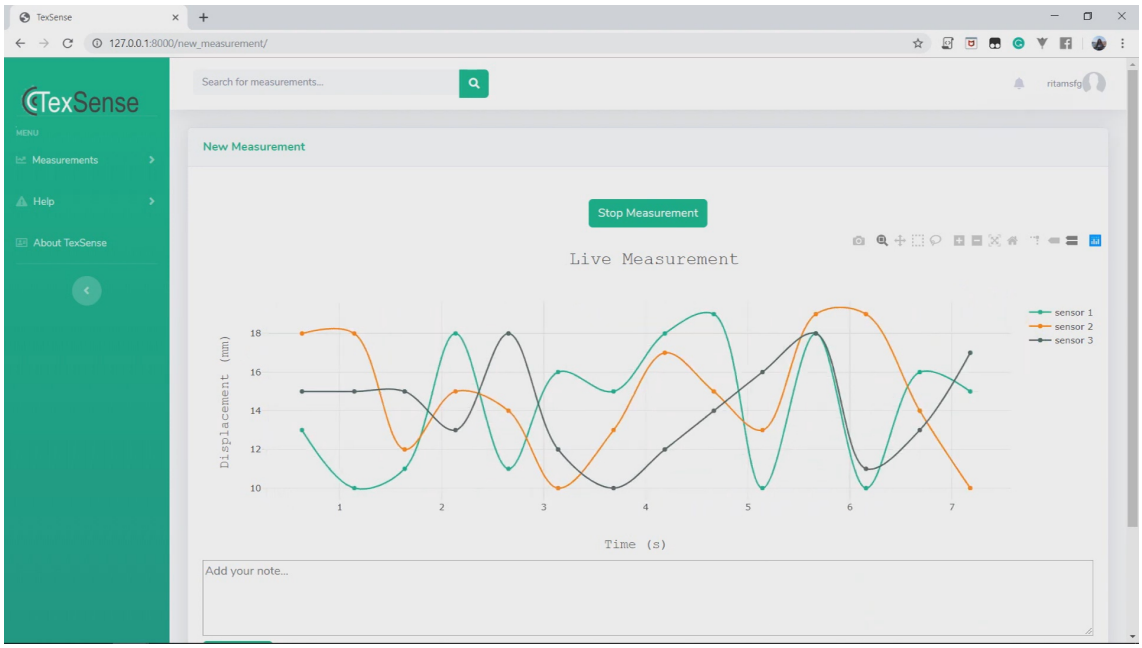

Figure 6.6: Live Measurement UI.

Figure 6.7: See performed Measurement UI.

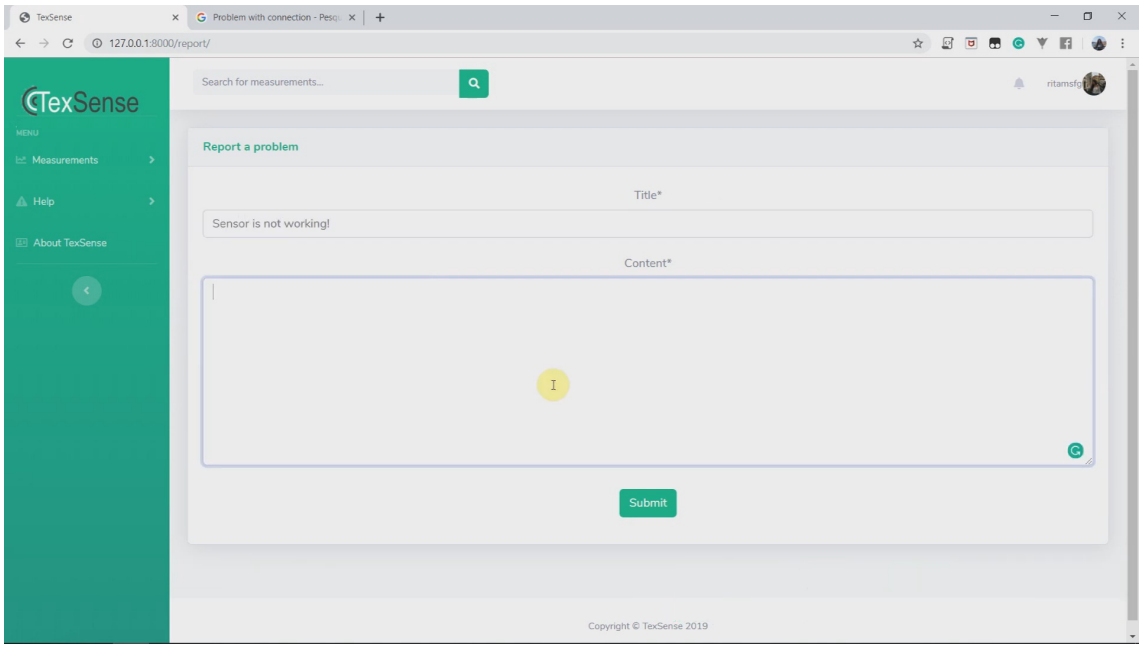

Figure 6.8: Create Report UI.

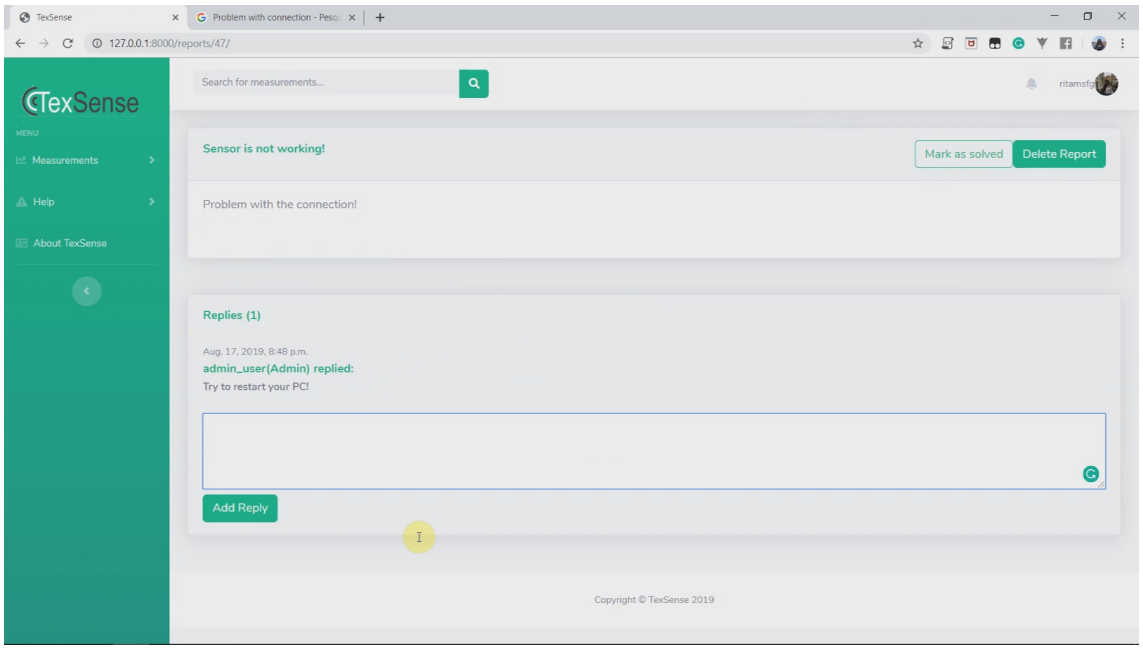

Figure 6.9: View Report UI.

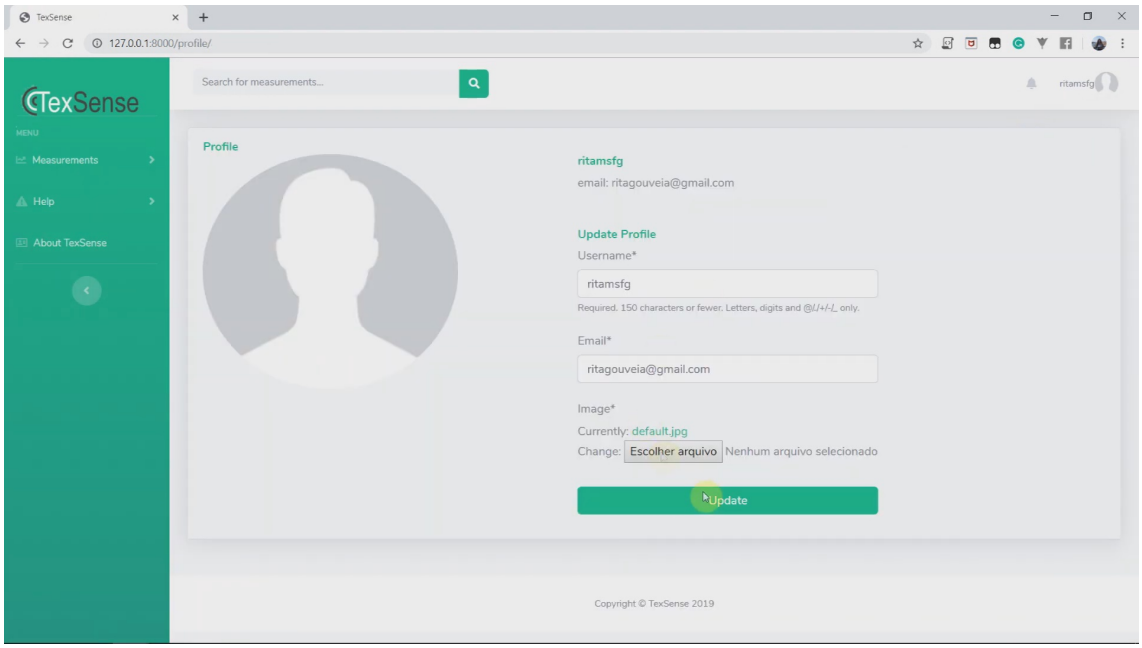

Figure 6.10: Profile UI.

not only the measurements in real-time but also all the performed ones. Finally, bearing in mind that users' feedback can have an added value in system enhancement, an additional section, where users can report their problems related to the system, was created.

Although the results were encouraging, a lot of enhancements need to be made, mainly if the goal is to develop a final product. In that case, some of the changes to be made would be, for example:

- Adding new features such as email verification and password reset;
- Acquiring the sensor output via Bluetooth instead of I^2C;
- Changing the database from SQLite to PostgreSQL since PostgreSQL has larger storage, handles multiple users, offers much more security, reliability, and extendability (SQLite is limited to basic operations) [3].

[3]More information at: https://tableplus.com/blog/2018/08/sqlite-vs-postgresql-which-database-to-use-and-why.html

Chapter 7

Conclusions

The development of a soft stretchable strain sensor was the principal goal of this dissertation. This process involved steps such as the selection of the material, design of the electronic circuit and the development of a web application prototype capable of communicating with the sensor.

The main contributions of this dissertation are:

- Research of existing strain sensors prototypes and commercially available solutions;
- Study of the behaviour of different textiles/materials when exposed to different displacements/strains;
- The textile carbon conductive paste based solution found that constitute an excellent option for a strain sensor;
- Design and test of two different circuits for signal aquisition and communication;
- Development of a web application prototype using Django, HTML, CSS and JavaScript that allows users to visualize the data acquired from the sensor in real-time and save the performed measurements.

7.1 Future Work

7.1.1 Perform different tests to the carbon conductive paste solution

Traction tests could be performed to the carbon conductive paste solution to evaluate its stretchability. It may also be interesting to expose the material to cyclic strains during long periods to study its durability under dynamic loads.

7.1.2 Test the influence of some properties of the carbon conductive paste solution

Change some properties in the conductive paste solution may desirably alter textile behaviour. For example, adding more conductive paste or modify the configuration can result in larger values of resistance.

7.1.3 Integrate the sensors into the wearable system

The sensor electronic circuit needs to be integrated into a flexible PCB and then glued properly to the wearable.

7.1.4 Test the strain sensor in an operational environment

The test performed to the textiles took placed in a controlled environment. As expected, the results in a real environment will be different, and the performance of the sensor is expected to be worst. Therefore, it is necessary to test the sensor in an operational environment and readjust it according to the test results.

7.1.5 Make the final product development and go-to-market plan

It may also be worth to have the option of selling the sensor separately. In this case, a fully functional app must communicate with the sensor. Therefore, some adjustments need to be performed to the web app prototype developed in this dissertation, as already discussed, to make it available on the market as well as the go-to-market plan.

Bibliography

[1] Stefan Schneegass and Oliver Amft. *Smart Textiles*. Springer, 2017.

[2] Mimi Shorr. Body covering : [catalog of an exhibition] april 6-june 9, 1968. New York : Museum of Contemporary Crafts of The American Craftsmen's Council, 1968, 1968.

[3] Tiago Fernández-Caramés and Paula Fraga-Lamas. Towards the internet-of-smart-clothing: A review on iot wearables and garments for creating intelligent connected e-textiles. *Electronics*, 7(12):405, 2018.

[4] Dusan Johnson. Smart shoes: Tracking fitness through your feet. https://gadgetsandwearables.com/2018/07/13/trackers-feet/, July 2018. Accessed: 2019-01-16.

[5] Sensoria. Sports bra + hrm. http://store.sensoriafitness.com/sports-bra-hrm/. Accessed: 2019-01-12.

[6] Rui Farinha. Coletes melhoram exibição dos craques do futebol. https://www.jn.pt/desporto/interior/coletes-melhoram-exibicao-dos-craques-9292447.html , April 2018. Accessed: 2019-01-14.

[7] Mozhdeh Ghahremani Honarvar and Masoud Latifi. Overview of wearable electronics and smart textiles. *The Journal of The Textile Institute*, 108(4):631–652, 2017.

[8] Biodevices S.A. Vital jacket: Catalogue. http://www.vitaljacket.com/wp-content/uploads/2017/07/VitalJacket_Catalog_2013.pdf, August 2018. Accessed: 2019-02-03.

[9] Márcia Raquel Estima Saraiva. VitalSleep: Wearable sleep device for ambulatory sleep quality monitoring. Master's thesis, Faculdade de Engenharia da Universidade do Porto, 2018.

[10] StatSports. Statsports. https://statsports.com/. Accessed: 2019-01-11.

[11] Yang Lu, Manik Chandra Biswas, Zhanhu Guo, Ju-Won Jeon, and Evan K Wujcik. Recent developments in bio-monitoring via advanced polymer nanocomposite-based wearable strain sensors. *Biosensors and Bioelectronics*, 2018.

[12] Magic Marks. Definition of poisson's ratio - magic marks, September 2013. URL https://www.youtube.com/watch?v=hBnzrBhnzVo. Accessed: 2019-01-18.

[13] Xinlei Shi, Huike Wang, Xueting Xie, Qingwen Xue, Jingyu Zhang, Siqi Kang, Conghui Wang, Jiajie Liang, and Yongsheng Chen. Bioinspired ultrasensitive and stretchable mxene-based strain sensor via nacre-mimetic microscale "brick-and-mortar" architecture. *ACS nano*, 2018.

[14] Andreas Frutiger, Joseph T Muth, Daniel M Vogt, Yiğit Mengüç, Alexandre Campo, Alexander D Valentine, Conor J Walsh, and Jennifer A Lewis. Capacitive soft strain sensors via multicore–shell fiber printing. *Advanced Materials*, 27(15):2440–2446, 2015.

[15] Morteza Amjadi and Inkyu Park. Carbon nanotubes-ecoflex nanocomposite for strain sensing with ultra-high stretchability. In *Micro Electro Mechanical Systems (MEMS), 2015 28th IEEE International Conference on*, pages 744–747. IEEE, 2015.

[16] Le Cai, Li Song, Pingshan Luan, Qiang Zhang, Nan Zhang, Qingqing Gao, Duan Zhao, Xiao Zhang, Min Tu, Feng Yang, et al. Super-stretchable, transparent carbon nanotube-based capacitive strain sensors for human motion detection. *Scientific reports*, 3:3048, 2013.

[17] Nuno Viriato Ramos Andreia Flores. Proposta de prestação de serviço para a realização de ensaios de tração em tecido condutor, 2018.

[18] *1 MSPS, 12-Bit Impedance Converter, Network Analyzer*. Analog Devices, 9 2005. Rev. F.

[19] *ADS111x Ultra-Small, Low-Power, I 2C-Compatible, 860-SPS, 16-Bit ADCs With Internal Reference, Oscillator, and Programmable Comparator*. Texas Instruments Incorporated, 5 2009. Rev. D.

[20] Bimlendu Roy. Microprocessor advantages disadvantages. https://www.techwalla.com/articles/microprocessor-advantages-disadvantages, May 2015. Accessed: 2019-01-10.

[21] Jonathan Rose, Robert J Francis, David Lewis, and Paul Chow. Architecture of field-programmable gate arrays: The effect of logic block functionality on area efficiency. *IEEE Journal of Solid-State Circuits*, 25(5):1217–1225, 1990.

[22] Advantages and disadvantages of an system on chip. https://www.thedailyprogrammer.com/2016/09/advantages-and-disadvantages-of-soc.html , September 2016. Accessed: 2019-01-16.

[23] Ascensión López-Vargas, Manuel Fuentes, and Marta Vivar. Iot application for real-time monitoring of solar home systems based on arduino^{TM} with 3g connectivity. *IEEE Sensors Journal*, 19(2):679–691, 2018.

[24] PF Silva Jr, RCS Freire, AJR Serres, PH da F Silva, and JC Silva. Wearable textile bioinspired antenna for 2g, 3g, and 4g systems. *Microwave and Optical Technology Letters*, 58 (12):2818–2823, 2016.

[25] Shahin Farahani. *ZigBee wireless networks and transceivers*. Newnes, 2011.

[26] Márcio Borgonovo-Santos João Paulo Vilas-Boas Hélder Rosendo Manuel Barros André Lemos Miguel Velhote Correia, Ana Florinda Ramôa. Pps1-an2 digitizaÇÃo e desmaterializaÇÃo de protÓtipos de vestuÁrio, october 2018.

[27] Ana M Grancarić, Ivona Jerković, Vladan Koncar, Cedric Cochrane, Fern M Kelly, Damien Soulat, and Xavier Legrand. Conductive polymers for smart textile applications. *Journal of Industrial Textiles*, page 1528083717699368, 2018.

[28] Md Syduzzaman, Sarif Ullah Patwary, Kaniz Farhana, and Sharif Ahmed. Smart textiles and nano-technology: a general overview. *J. Text. Sci. Eng*, 5:1000181, 2015.

[29] HLEEWAINWRIGHT. H. lee wainwright: The grandfather of e-textiles. http://www.hleewainwright.com/, April 2014. Accessed: 2019-01-12.

[30] Jonny Farringdon, Andrew J Moore, Nancy Tilbury, James Church, and Pieter D Biemond. Wearable sensor badge and sensor jacket for context awareness. In *Wearable Computers, 1999. Digest of Papers. The Third International Symposium on*, pages 107–113. IEEE, 1999.

[31] Corinne Mattmann, Oliver Amft, Holger Harms, Gerhard Troster, and Frank Clemens. Recognizing upper body postures using textile strain sensors. In *Wearable Computers, 2007 11th IEEE International Symposium on*, pages 29–36. IEEE, 2007.

[32] Gilsoo Cho, Keesam Jeong, Min Joo Paik, Youngeun Kwun, and Moonsoo Sung. Performance evaluation of textile-based electrodes and motion sensors for smart clothing. *IEEE Sensors Journal*, 11(12):3183–3193, 2011.

[33] Tien-Wei Shyr, Jing-Wen Shie, Chang-Han Jiang, and Jung-Jen Li. A textile-based wearable sensing device designed for monitoring the flexion angle of elbow and knee movements. *Sensors*, 14(3):4050–4059, 2014.

[34] Rita Paradiso, Giannicola Loriga, and Nicola Taccini. A wearable health care system based on knitted integrated sensors. *IEEE transactions on Information Technology in biomedicine*, 9(3):337–344, 2005.

[35] O Amft and J Habetha. Smart medical textiles for monitoring patients with heart conditions. *Smart Textiles for Medicine and Healthcare Materials, Systems and Applications. Woodhead Publishing Limited: Cambridge, England*, pages 275–301, 2007.

[36] Samjin Choi and Zhongwei Jiang. A wearable cardiorespiratory sensor system for analyzing the sleep condition. *Expert Systems with Applications*, 35(1-2):317–329, 2008.

[37] Kunigunde Cherenack and Liesbeth van Pieterson. Smart textiles: Challenges and opportunities. *Journal of Applied Physics*, 112(9):091301, 2012.

[38] Stefano Maddio, Alessandro Cidronali, and Gianfranco Manes. Rssi/doa based positioning systems for wireless sensor network. In *New Approach of Indoor and Outdoor Localization Systems*. InTech, 2012.

[39] Sam Lemey, Sam Agneessens, Patrick Van Torre, Kristof Baes, Jan Vanfleteren, and Hendrik Rogier. Wearable flexible lightweight modular rfid tag with integrated energy harvester. *IEEE Transactions on Microwave Theory and Techniques*, 64(7):2304–2314, 2016.

[40] Javad Foroughi, Teodor Mitew, Philip Ogunbona, Raad Raad, and Farzad Safaei. Smart fabrics and networked clothing: Recent developments in cnt-based fibers and their continual refinement. *IEEE Consumer Electronics Magazine*, 5(4):105–111, 2016.

[41] Xuetao Wei, Lorenzo Gomez, Iulian Neamtiu, and Michalis Faloutsos. Permission evolution in the android ecosystem. In *Proceedings of the 28th Annual Computer Security Applications Conference*, pages 31–40. ACM, 2012.

[42] Abhinav M Gaikwad, Ana Claudia Arias, and Daniel A Steingart. Recent progress on printed flexible batteries: mechanical challenges, printing technologies, and future prospects. *Energy Technology*, 3(4):305–328, 2015.

[43] Weiqing Yang, Jun Chen, Guang Zhu, Jin Yang, Peng Bai, Yuanjie Su, Qingsheng Jing, Xia Cao, and Zhong Lin Wang. Harvesting energy from the natural vibration of human walking. *ACS nano*, 7(12):11317–11324, 2013.

[44] Vladimir Leonov. Thermoelectric energy harvesting of human body heat for wearable sensors. *IEEE Sensors Journal*, 13(6):1–8, 2013.

[45] Zhisheng Chai, Nannan Zhang, Peng Sun, Yi Huang, Chuanxi Zhao, Hong Jin Fan, Xing Fan, and Wenjie Mai. Tailorable and wearable textile devices for solar energy harvesting and simultaneous storage. *ACS nano*, 10(10):9201–9207, 2016.

[46] Michael A Leabman and Gregory Scott Brewer. Wireless charging of clothing and smart fabrics, June 11 2015. US Patent App. 14/103,528.

[47] Nick Wright. Statsports: The training technology used by arsenal, man city, barcelona and more. https://www.skysports.com/football/news/11095/10502787/statsports-the-training-technology-used-by-arsenal-man-city-barcelona-and-more , July 2016. Accessed: 2019-01-14.

[48] Biodevices S.A. Instituto de telecomunicações cria sistema de monitorização dos sinais vitais dos bombeiros. http://www.vitaljacket.com/pt/instituto-de-telecomunicacoes-cria-sistema-de-monitorizacao-dos-sinais-vitais-dos-bombeiros/, February 2018. Accessed: 2019-02-02.

[49] Daniel Rubino. Ie9 for windows phone 7: Adobe flash, demos and development. http://www.wpcentral.com/ie9-windows-phone-7-adobe-flash-demos-and-development-videos, February 2011. Accessed: 2019-01-18.

[50] Duarte Filipe Dias. VitalLogger: An Adaptable Wearable Physiology and Ambiance Data Logger for Mobile Applications. Master's thesis, Faculdade de Engenharia da Universidade do Porto, 2015.

[51] Hexoskin. Hexoskin online store. https://www.hexoskin.com/collections/all, 2019. Accessed: 2019-10-19.

[52] Theodore Hughes-Riley, Tilak Dias, and Colin Cork. A historical review of the development of electronic textiles. *Fibers*, 6(2):34, 2018.

[53] Deborah Weinswig. THE WEARABLES REPORT 2016: REVIEWING A FAST-CHANGING MARKET. Technical report, Fung Global Retail And Technology, 06 2016.

[54] Paul Lamkin. Wearable tech market to be worth $34 billion by 2020. https://www.forbes.com/sites/paullamkin/2016/02/17/wearable-tech-market-to-be-worth-34-billion-by-2020/#eca16ed3cb55, February 2016. Accessed: 2019-01-10.

[55] James Hayward. E-textiles 2018-2028: Technologies, markets and players. https://www.idtechex.com/research/reports/e-textiles-2018-2028-technologies-markets-and-players-000613.asp, July 2018. Accessed: 2019-01-11.

[56] Morteza Amjadi, Ki-Uk Kyung, Inkyu Park, and Metin Sitti. Stretchable, skin-mountable, and wearable strain sensors and their potential applications: a review. *Advanced Functional Materials*, 26(11):1678–1698, 2016.

[57] Hamid Souri and Debes Bhattacharyya. Highly sensitive, stretchable and wearable strain sensors using fragmented conductive cotton fabric. *Journal of Materials Chemistry C*, 6(39): 10524–10531, 2018.

[58] Heng Yang, XueFeng Yao, Zhong Zheng, LingHui Gong, Li Yuan, YaNan Yuan, and YingHua Liu. Highly sensitive and stretchable graphene-silicone rubber composites for strain sensing. *Composites Science and Technology*, 167:371–378, 2018.

[59] Yalong Wang, Yanyan Jia, Yujie Zhou, Yan Wang, Guoqiang Zheng, Kun Dai, Chuntai Liu, and Changyu Shen. Ultra-stretchable, sensitive and durable strain sensors based on polydopamine encapsulated carbon nanotubes/elastic bands. *Journal of Materials Chemistry C*, 6(30):8160–8170, 2018.

[60] Minxuan Xu, Junjie Qi, Feng Li, and Yue Zhang. Highly stretchable strain sensors with reduced graphene oxide sensing liquids for wearable electronics. *Nanoscale*, 10(11):5264–5271, 2018.

[61] Ung-Hui Shin, Dong-Wook Jeong, Sang-Min Park, Soo-Hyung Kim, Hyung Woo Lee, and Jong-Man Kim. Highly stretchable conductors and piezocapacitive strain gauges based on simple contact-transfer patterning of carbon nanotube forests. *Carbon*, 80:396–404, 2014.

[62] Xi Fan, Naixiang Wang, Jinzhao Wang, Bingang Xu, and Feng Yan. Highly sensitive, durable and stretchable plastic strain sensors using sandwich structures of pedot: Pss and an elastomer. *Materials Chemistry Frontiers*, 2(2):355–361, 2018.

[63] Q Li, K Wang, Y Gao, JP Tan, RY Wu, and FZ Xuan. Highly sensitive wearable strain sensor based on ultra-violet/ozone cracked carbon nanotube/elastomer. *Applied Physics Letters*, 112 (26):263501, 2018.

[64] Xu Liu, Dan Liu, Jeng-hun Lee, Qingbin Zheng, Xiaohan Du, Xinyue Zhang, Hongru Xu, Zhenyu Wang, Ying Wu, Xi Shen, et al. Spider web-inspired stretchable graphene woven fabric for highly sensitive, transparent, wearable strain sensors. *ACS applied materials & interfaces*, 2018.

[65] Jeffrey G Dabling, Anton Filatov, and Jason W Wheeler. Static and cyclic performance evaluation of sensors for human interface pressure measurement. In *Engineering in Medicine and Biology Society (EMBC), 2012 Annual International Conference of the IEEE*, pages 162–165. IEEE, 2012.

[66] Hae-Jin Kim, Anish Thukral, and Cunjiang Yu. Highly sensitive and very stretchable strain sensor based on a rubbery semiconductor. *ACS applied materials & interfaces*, 10(5):5000–5006, 2018.

[67] Hyungdong Lee, Baekhoon Seong, Hyungpil Moon, and Doyoung Byun. Directly printed stretchable strain sensor based on ring and diamond shaped silver nanowire electrodes. *Rsc Advances*, 5(36):28379–28384, 2015.

[68] Yichen Cai, Jie Shen, Gang Ge, Yizhou Zhang, Wanqin Jin, Wei Huang, Jinjun Shao, Jian Yang, and Xiaochen Dong. Stretchable ti3c2t x mxene/carbon nanotube composite based strain sensor with ultrahigh sensitivity and tunable sensing range. *ACS nano*, 12(1):56–62, 2017.

[69] Inhyuk Kim, Kyoohee Woo, Zhaoyang Zhong, Pyungsam Ko, Yunseok Jang, Minhun Jung, Jeongdai Jo, Sin Kwon, Seung-Hyun Lee, Sungwon Lee, et al. A photonic sintering derived ag flake/nanoparticle-based highly sensitive stretchable strain sensor for human motion monitoring. *Nanoscale*, 10(17):7890–7897, 2018.

[70] Xin Wang, Jinfeng Li, Haonan Song, Helen Huang, and Jihua Gou. Highly stretchable and wearable strain sensor based on printable carbon nanotube layers/polydimethylsiloxane composites with adjustable sensitivity. *ACS applied materials & interfaces*, 10(8):7371–7380, 2018.

[71] Kang-Hyun Kim, Nam-Su Jang, Sung-Hun Ha, Ji Hwan Cho, and Jong-Man Kim. Highly sensitive and stretchable resistive strain sensors based on microstructured metal nanowire/elastomer composite films. *Small*, 14(14):1704232, 2018.

[72] Asli Atalay, Vanessa Sanchez, Ozgur Atalay, Daniel M Vogt, Florian Haufe, Robert J Wood, and Conor J Walsh. Batch fabrication of customizable silicone-textile composite capacitive strain sensors for human motion tracking. *Advanced Materials Technologies*, 2(9):1700136, 2017.

[73] Ozgur Atalay, Asli Atalay, Joshua Gafford, Hongqiang Wang, Robert Wood, and Conor Walsh. A highly stretchable capacitive-based strain sensor based on metal deposition and laser rastering. *Advanced Materials Technologies*, 2(9):1700081, 2017.

[74] Shanshan Yao and Yong Zhu. Wearable multifunctional sensors using printed stretchable conductors made of silver nanowires. *Nanoscale*, 6(4):2345–2352, 2014.

[75] Daniel J Cohen, Debkishore Mitra, Kevin Peterson, and Michel M Maharbiz. A highly elastic, capacitive strain gauge based on percolating nanotube networks. *Nano letters*, 12(4): 1821–1825, 2012.

[76] *Bend Sensor® Technology Electronic Interface Design Guide*. Flexpoint, 2015.

[77] I-CubeX. Bendshort v2.0. https://infusionsystems.com/catalog/product_info.php/products_id/54, March 2018. Accessed: 2019-04-05.

[78] *Stretch Sensing Element*. *StretchSense*^{TM}, 2018.

[79] *Stretch Sensing Element*. Spectrasymbol, 2014.

[80] Tinkersphere. Stretch sensor. https://tinkersphere.com/sensors/2405-stretch-sensor.html, April 2019. Accessed: 2019-04-04.

[81] Sal Afzal. I2c primer: What is i2c? (part 1). https://www.analog.com/en/technical-articles/i2c-primer-what-is-i2c-part-1.html, 2019. Accessed: 2019-07-29.

[82] Il-Yeol Song and K Froehlich. Entity-relationship modeling. *Potentials, IEEE*, 13:29 – 34, 02 1995. doi: 10.1109/45.464652.

[83] André Restivo. Relational model, February 2013.